THE UNIVERSITY OF ALBERTA

INFLUENCE OF GAS ENVIRONMENTS ON FATIGUE OF COPPER

by

© GUSTAV SIDLA

A THESIS

SUBMITTED TO THE FACULTY OF GRADUATE STUDIES

IN PARTIAL FULFILMENT OF THE REQUIREMENTS FOR THE DEGREE

OF MASTER OF SCIENCE

IN METALLURGICAL ENGINEERING

DEPARTMENT OF MINING AND METALLURGY

EDMONTON, ALBERTA

FALL, 1970

THE UNIVERSITY OF ALBERTA

FACULTY OF GRADUATE STUDIES

The undersigned certify that they have read, and recommend to the Faculty of Graduate Studies for acceptance, a thesis entitled

INFLUENCE OF GAS ENVIRONMENTS ON FATIGUE OF COPPER

submitted by GUSTAV SIDLA

in partial fulfilment of the requirements for the degree of Master of Science.

Date October 22, 1970

ABSTRACT

The effect of gaseous environment and irradiation by low energy particles on the fatigue life of O.F.H.C. copper was studied in reversed bending at constant strain amplitude. Gases used in this project were oxygen, hydrogen, nitrogen, argon and helium at reduced pressures. Specimens were irradiated by ions and by electrons respectively having energies of 450 ev.

The environmental sensitivity of copper was confirmed. The fatigue life was increased in the sequence oxygen, hydrogen, nitrogen, argon, helium according to the amount of oxygen present as impurity thus verifying that oxygen is the determining element in the environment. Electron microscopy showed that the fatigue crack initiation was little influenced by the environment. Rather, the observed effect of environment on the fatigue life is related to stage I crack propagation.

Ionization of the gases causes additional enhancement of the effects of the environment with exception of hydrogen where presumably a reduction in residual content of oxygen due to formation of water takes place.

Observed preferential oxidation in the slip bands supports the rewelding theory of interaction between oxygen and the solid. It is believed that rewelding is complemented by a brittle-film rupture mechanism.

Even though the mixed intercrystalline-transcrystalline mode of fracture is always found, the fracture topography reflects the effect of environment to some extent.

ACKNOWLEDGEMENTS

The author is indebted to Dr. F.H. Vitovec for his invaluable help and kind assistance throughout the project.

The research for this thesis was supported by the Defence Research Board of Canada, Grant number 9535-40. This support is greatly appreciated by the author.

TABLE OF CONTENTS

TABLE OF CONTENTS (cont'd)

LIST OF TABLES

LIST OF FIGURES

LIST OF FIGURES (cont'd)

LIST OF FIGURES (cont'd)

1. INTRODUCTION

Failures occuring under conditions of cyclic loading are termed fatigue failures. In contrast to failure due to an overload, fatigue failures occur at stresses which are lower than the yield strength. Fatigue failures have been observed in many materials and account for at least 90 per cent of all mechanical failures in service.

By studying the fatigue behavior in laboratories some fatigue characteristics are usually determined. One of the most used characteristics of fatigue of metal is the fatigue life which is defined as the number of cycles to failure at given cycling stress or strain amplitude. The fatigue life is usually regarded as consisting of three stages. The first stage is termed fatigue crack nucleation. In smooth specimens the nucleation involves initiation of cracks in slip bands or other regions of strain localization and is controlled by shear stresses. The crack nucleation in smooth specimens of ductile metals is generally completed after less than 10 per cent of their total life (1). The crack nucleation period is succeeded by the stage I crack propagation. Stage I crack propagation entails deepening of the initial crack on planes of high shear stress. This mode of propagation may be absent in acutely notched, highly stressed specimens, yet it may involve up to 90 per cent of the total cycles to failure. As the crack moves from a free surface

into the interior of a specimen, slip becomes difficult. The crack propagation is then controlled by the stress intensity at the crack tip and takes place on planes of maximum tensile stress. This mode of crack growth is designated "stage II crack propagation" and may occupy from 10 per cent to 100 per cent of the fatigue life of a specimen (1).

Since the fatigue damage usually starts at the surface, the state of the surface plays an important part in determining the fatigue behavior. Furthermore, interaction between the environment and the bulk of the material takes place on the surface. Therefore, the fatigue of materials is extremely sensitive to the environment. The significance of the surface in fatigue processes is well documented by fatigue tests done by Kramer (2). He performed tests on an aluminium alloy and by impregnating the porous anodized coating with polar organic molecules he obtained a remarkable increase of the fatigue life. The most active impregnant was palmitic acid which resulted in an increase of the fatigue life by two orders of magnitude with respect to fatigue life obtained with an untreated specimen. Similarly a wide variety of organic materials such as acids, amines, and alcohols were found to be effective in improving the fatigue strength. However, materials which do not have an active polar group exerted little or no effect on the fatigue life.

Other forms of surface treatment proved to be effective too. Application of film-forming liquids extended the fatigue life of

steel (3, 4). Coating with butyl rubber increased the fatigue life of aluminium alloy specimens (5).

Gaseous environments can influence the fatigue behavior of metals as well. It is well known that a reduction of the pressure of air results in an increase of the fatigue life. For example, reduction of the air pressure to 10^{-5} torr increased the fatigue life of copper by a factor of 20 (6). The mechanisms proposed to explain the beneficial effect of chemical surface treatments and of vacuum respectively have one thing in common; they are all based on the assumption that oxygen is prevented to reach the tip of the crack.

In regard to the effect of gaseous environments on the fatigue of metals, the most complete information is available for aluminium and its alloys (3, 5, 7, 8, 9, 10, 11, 12). The effect of environment on fatigue of copper has not been studied to such extent (6, 13, 14). Even though many studies were performed on engineering materials in an attempt to clarify the environmental effects there are still some contradictions as will be shortly described.

There are some doubts with respect to the extent of the environmental influence on the fatigue crack nucleation. Grosskreutz and Bowles (10) found by studying the surface deformation of aluminium and gold that formation of slip bands was greatly suppressed at 10^{-9} torr. This would affect the fatigue crack nucleation which is a consequence of slip. However, they did not analyse their results from the point of view of crack nucleation. Earlier, Broom and

Nicholson (5) found on aluminium that cracks occured sooner in air than in vacuum. This led them to conclude that crack initiation was affected more than growth. Bradshaw and Wheeler (12) arrived at the opposite conclusion from the finding that the fatigue life of notched specimens of an aluminium alloy was affected more by the environment than the fatigue life of plain specimens. Laird and Smith (15) working with nickel demonstrated that cracks were present in the early stages in vacuum and that the effect of environment on the fatigue life can be attributed to a difference in crack propagation rate. Recently Grosskreutz (16) reported that crack nuclei were formed earlier in oxygen than in vacuum.

The mechanisms of the effect of oxygen are not as yet clarified either. There are two possible ways in which oxygen can assist crack propagation. It might attack the highly strained material at the crack tip and so weaken it or it might form an oxide layer on freshly exposed surfaces preventing the crack rewelding during the compressive part of the cycle. Martin (17) found some reweldment of the crack surfaces in stainless steel, copper and aluminium tested in vacuum of 10^{-6} torr. Similarly Frost (4), on the basis of his observations, concluded that there was some re-bonding of the freshly created surfaces at the crack tip during the compression half of the loading cycle in the absence of oxygen. The rewelding theory was criticized by Laird and Smith (15). Since they found no evidence for welding of the cracks they favor the corrosive attack hypothesis.

Much effort has been devoted to the explanation of S-shaped curves of gas pressure versus fatigue life or crack propagation rate. The salient features of the S-shaped curves are two plateaus, along which the fatigue properties are independent of gas pressure and the transition region where the properties are decreased with increasing pressure. Achter (18) explains the shape of the curves as follows. The crack growth rate increases with increasing pressure until a critical pressure is reached at which the surface is saturated with gas in a time equal to half the period of vibration. Once a monolayer is formed there is no further effect of increase in gas pressure.

The critical pressure is around 10^{-1} torr. According to Grosskreutz (10) a monolayer of oxygen can still form in the very short time of 1 sec. at pressure around 10^{-6} torr and this is inconsistent with Achter's explanation. Furthermore, the S-shape does not apply for copper (6, 13). There is not a critical pressure of oxygen for copper. The behavior of copper can be explained well in terms of the brittle film hypothesis, though. The brittle oxide film which would be easily ruptured causing local stress concentration would make crack propagation easier. Since the thickness of the brittle oxide film produced on freshly formed surfaces is proportional to the oxygen pressure; the stress concentration and thus the crack propagation would be linearly related to the oxygen pressure. The brittle film formation has been proven to assist the stress corrosion cracking (19).

Even though many studies have been done to separate the effects of oxygen and water vapor there are still some doubts as to their influence. Wadsworth and Hutchings (6) reported that the life of copper in a vacuum of 7×10^{-6} torr was 20 times longer than in air. In dry air the ratio was about 10 but in wet oxygen it was approximately 30. However, in water vapor alone the life was about the same as in vacuum. They concluded that oxygen is the effective component in air and that water vapor increased the effect of oxygen. Snowden (20) working with lead, also found that oxygen was the damaging component, but its effect was not increased by water vapor. In case of aluminium and its alloys it is the water vapor which is the dominant factor. For example, in the alloy 2024-T3 there was no difference in the rate of fatigue crack propagation in wet air, wet argon and wet oxygen. In fact, cracking in wet argon was more severe than in dry, pure oxygen (12).

There is a general lack of information on fatigue processes in ionized gases and under irradiation by low energy ions and electrons. It is known that electrical discharge in gases can influence their composition. Recent investigation by Smith and Shahinian (21) is relevant. Evidence obtained by residual gas analysis showed that a hot ionization gage filament may change the composition of the environment which in turn, may affect the fatigue life. Furthermore, ozone can be readily formed in electrical discharges (22). Since the reactivity of ozone is superior

to that of oxygen a reduction of fatigue life is to be anticipated in environments containing ozone.

Material subjected to irradiation by ions suffers from sputtering. The term sputtering is used for a phenomenon of removal of the surface atoms due to the collisions with positive ions. Sputtering has recently become of importance with space flights as it was feared that the damage to the rockets and satellites would be severe. Questions arise when one considers the lack of study of sputtering accompanied by formation of ozone with respect to fatigue properties.

Fatigue damage normally occurs by slip band cracking at the surface which propagates in stage I not only along the surface but also penetrates into the material. It has been shown that intermittent removal of this damaged layer increases the fatigue life (23). Sputtering which causes essentially the removal of a surface layer might influence the fatigue behavior in a similar way. However, there are basically three processes and their relative rates which determine the effect of ionizing radiation on fatigue. The relative rate of the chemical interaction, that of fatigue damage as well as that of removal of the fatigue damaged layer may determine whether or not the fatigue life is increased or decreased.

From this short review it can be seen that many aspects of the effect of the gaseous environments on metal fatigue require further study. This project was undertaken in an attempt to

clarify some of the questions, namely:

- to clarify the effect of different gases on crack nucleation,
- to clarify the extent of the effect of environment on stage I and stage II crack propagation,
- to clarify which one of the proposed mechanisms (corrosive attack, rewelding or brittle-film formation) is dominant,
- to verify the effect of water vapor on crack propagation and fatigue life,
- to investigate the influence of ionization of gases on the rate of environmental effects,
- to investigate the effect of irradiation by ions and electrons respectively on the fatigue life,
- to investigate whether it is the removal of a layer due to sputtering or the increased rate of chemical reaction which determines the fatigue life under irradiation by ions,
- to investigate the modes of oxidation under irradiation by oxygen ions.

2. EXPERIMENTAL PROGRAM AND PROCEDURES

2.1 Experimental Program

To study the environmental effects and gain information on the previously outlined questions the following testing program and test conditions were selected:

1. Reversed bending fatigue tests at constant amplitude to study the effect of differences in the environment on the fatigue life.
2. O.F.H.C. copper was selected as test material because extensive information on its fatigue behavior is available from the literature and film formation due to reactions can more easily be observed because of color changes.
3. Gases for the environments used were oxygen, nitrogen, hydrogen, argon and helium.
4. The tests were performed at pressures of 45 torr and at 0.1 torr to compare with tests under irradiation conditions which require reduced pressures. Furthermore, information on the pressure dependence of the fatigue life is obtained.
5. In some test series a glow discharge was produced to cause ionization of the environmental gases and to increase the probability and the rate of interaction with the test specimen. This glow discharge was directed so that the specimens were irradiated either by ions or electrons. The irradiation conditions were as follows:

(a) the specimens were made one of the two electrodes so that the ionization processes were taking place in close vicinity to the specimen surface; furthermore, by changing the polarity the specimen surface was irradiated by ions or electrons.

(b) the specimens were irradiated by ions produced in an ion gun providing a different chemical environment and weaker sputtering effect.

Information on the effects of the environmental conditions on the fatigue properties was obtained from the following experimental data and techniques:

1. Fatigue life.
2. Frequency change which gives information on crack propagation.
3. Electron microscopy for information on crack propagation.
4. Visible light microscopy and color photography for information on oxide formation, oxide growth and slip.
5. Electron fractography to study the effect of environment on the characteristics of crack propagation and other details of the fracture surface.

2.2 Description of Testing Apparatus

Fatigue testing was performed in a resonance type reversed bending fatigue machine. Fig. 1 and Fig. 2 serve to illustrate the experimental apparatus. The fatigue machine permits reversed

bending of sheet metal specimens. The bottom part of the specimen is mounted in a specimen grip. The top part is connected to an extension arm forming this way a vibrating reed which operates at resonant frequency. The system is excited to vibrations and the vibration amplitude is maintained constant by electromagnets which are switched through contacts on the extension arm. A transistorized electrical feedback circuit keeps the specimen at resonance. The vibration amplitude is monitored by a linear variable differential transformer (LVDT) in conjunction with a transducer-amplifier. This signal is used to record the frequency and the vibration amplitude. Spot reading and calibration of the frequency is provided by a counter which is connected into the circuit. The amplitude of vibration is transmitted on the screen of an oscilloscope. Provision is made for automatic switch-off of the entire electrical supply at specimen failure. As a crack develops the frequency of amplitude is reduced, and the test is terminated when the frequency reaches a preset value. The bending amplitude changes very little throughout the test so that manual resetting is sufficient to maintain it constant. To minimize magnetic interference and contact with the environment in the test chamber both the magnets and the differential transformer are shielded and encapsulated in a metal can. The apparatus is placed in a vacuum chamber capable of producing a vacuum of 10^{-6} torr.

The vacuum chamber itself consists of a steel cylinder, stainless steel base plate and an aluminium top plate with a glass window. A vacuum diffusion pump is attached to the base plate. To minimize the oil vapor entering the chamber a water cooled plate valve and a water cooled chevron baffle is incorporated between the chamber and the diffusion pump. The gauge head of the ionization vacuum gauge is located in the test chamber near the specimen. For tests at selected reduced pressures the vacuum is maintained through a manually controlled leak-in valve.

Ionization of gases and irradiation of the specimen surface was done by two methods. In the first case a copper wire with a flat polished tip of 2.5 mm diameter connected to a high voltage terminal placed on the wall of the steel cylinder is positioned at a distance of 2 mm from the specimen surface. Application of a high voltage (450v) to the electrode and the test specimen at reduced gas pressures (45torr) causes ionization and bombardment of the test specimen by either electrons or ions, depending on the polarity which is applied.

As a second source of irradiation, a device called ion gun was used. A detailed description of the ion gun can be found in reference (24). A simplified diagram of the ion gun is shown in Fig. 3. The ion gun consists of a cylindrical anode, a cathode and a cathode grill. A potential drop of 2000v at pressure of 0.1torr causes an ionization in the gun; ions forming a jet passing through the cathode grill and striking the specimen surface. The

ion gun is connected to a high voltage terminal placed on the wall of the cylinder of the vacuum chamber. A d-c power supply provides the voltage necessary for operation.

2.3 Specimen Preparation

The test specimens were prepared from an oxygen free high conductivity (O.F.H.C.) copper bar of 3/4 in. diameter. Data from the spectrographic analysis are given in Table 1. The bar was cold rolled in steps to a strip 0.055 in. thick. Each cold rolling step was followed by annealing at 640°C for an hour in an argon atmosphere. After the last rolling operation the specimens were machined to a shape and size as shown in Fig. 4. The specimens were then polished down to the final thickness of 0.050 in. on a set of emery papers finishing with 600 grit. After polishing the specimens were annealed for one hour in argon at 640°C giving the average grain size of 0.045 mm. Immediately before mounting in the testing machine, the specimens were chemically polished in a bath composed of 55 per cent orthophosphoric acid, 25 per cent acetic acid and 20 per cent nitric acid. This was done by immersing the specimen for 15 sec. in the polishing solution preheated to 65°C.

2.4 Testing Procedure

After mounting the test specimen in the vibrator and adjustment of the electrical contacts the vacuum chamber was closed and

a vacuum in the range of 2×10^{-6} torr to 5×10^{-6} torr produced. The vacuum chamber was then purged twice with the gas of the test environment and the final vacuum adjusted to the pressure necessary to form the discharge. The gases used were argon, helium, hydrogen, nitrogen and oxygen. They were of high purity grade and a specification of impurities for every gas is given in Table 2 as supplied by the manufacturer. The pressure of 45 torr (for discharge between an electrode and the specimen) and 0.1 torr (for ionization by the ion gun) was kept constant by a controlled flow of gas through the chamber regulated by a calibrated leak-in valve. Testing in gases without ionization was performed at the same pressure as with ionization (i.e. 45 torr and 0.1 torr respectively) to obtain comparable data. The vibration amplitude was kept the same for all tests. It was maintained constant throughout the tests by manual adjustments. In spite of the use of voltage stabilizers line voltage variations caused small steps in the recordings. However, the variation of the vibration amplitude was in all cases smaller than 5 per cent. The frequency of vibration was recorded throughout the tests. In addition, spot readings of frequency on an electronic counter were taken at regular intervals to complement the calibration.

To ascertain the effect of heating by the electron or ion beams a specially prepared specimen with an embedded thermocouple was used. The maximum operating temperature due to charged particle bombardment was 34°C.

For tests in which the effect of humidity was studied, dessicated and humidified air were used. These tests were performed at atmospheric pressure. The dessicated air was obtained by covering the bottom of the testing chamber with dishes containing fresh silica gel. The resulting content of moisture in the chamber was less than one per cent relative humidity. For the humidified air the silica gel was replaced by tap water and this way 96 per cent relative humidity was obtained.

2.5 Calibration

The fatigue machine was calibrated for strain and load as a function of deflection. A sample test specimen with a strain gauge attached to the surface was mounted in the vibrator. A series of measurements was taken to obtain a calibration curve for deflection and corresponding strain. Then a set of weights attached to the vibration reed in horizontal position was used to produce a calibration for strain as a function of load. From there it was possible to calculate the load (stress) for a given deflection corresponding to a certain strain. The amplitude of vibration which resulted in a strain of $1.85\ 10^{-3}$ in. per in. was selected to give fatigue failure within a reasonable period of time. Although the amplitude of vibration was the same in all tests, there were some variations in stress and strain due to dimensional deviations of the test specimens.

2.6 Replication Technique for Electron Microscopy

To facilitate the observation of both fracture and free surfaces two-stage replicas were used. Preparation of a two-stage replica involves pressing a plastic replicating tape softened in acetone against the surface which is to be observed. After the replicating tape has hardened, which usually takes about five minutes, it is stripped from the surface. The tape is then placed into a vacuum evaporator where a layer of shadowing metal (palladium) is deposited under an angle of approximately 45 degrees. Then a carbon layer is deposited perpendicular to the surface of the tape. The tape is then cut to size and the plastic is dissolved in acetone. The replica is placed on a copper grid and dried; it is then ready for observation in the electron microscope.

3. TEST RESULTS

Testing in reversed bending in different gas environments confirmed differences in fatigue life of OFHC copper. The number of specimens tested in each of the environments was rather small so that statistically sound data cannot be obtained. However, in most instances the effect of gases is greater than the scatter and thus a certain trend is expressed by the results. The testing in all the gases was done at the pressure of a self sustaining glow discharge (45 torr) or at the pressure of the ion beam (0.1 torr) to have a possibility of comparing data. As will be discussed later, a series of tests for each environment was done under irradiation caused by the glow discharge and under bombardment by the ion beam.

3.1 Tests at Reduced Pressure Without Irradiation

A summary of data obtained by testing in different environments is presented in Table 3. The fatigue lives are plotted in the diagram shown in Fig. 5.

The shortest fatigue life was found in oxygen. This indicates that oxygen is the most active gas as far as the fatigue damage is concerned. Although some scatter occurs (i.e. from 0.95 to 1.45 million cycles) the fatigue life is definitely the shortest among those tested in the different environments.

The fatigue lives in hydrogen ranged from 1.10 to 1.60 million cycles which is slightly higher than in oxygen. Following hydrogen is nitrogen which resulted in 1.65 million cycles to failure. The cycles to failure in argon ranged from 1.7 to 2.5 million.

The most striking increase in fatigue life was found when a helium atmosphere was used as a testing environment. The number of cycles to failure increased to 5.92 million cycles, which is more than four times better than that in oxygen and more than two times better than that in argon. This sequence is similar to that observed by other investigators for tests at atmospheric pressure (25).

The high fatigue life in helium is believed to be partially due to the fact that the purity of the helium gas was superior to all other gases used. In particular the residual content of oxygen which plays a very important part in determining the fatigue behavior of copper was low (see Table 2).

To verify the effect of moisture on the number of cycles to failure, several tests were performed in dessicated air (less than one per cent relative humidity) and in humidified air (96 per cent relative humidity) at atmospheric pressure. Fig. 7 shows that the difference was rather small representing a change of 9 per cent only. This suggests that the moisture is not the important factor in the fatigue life of copper. Nevertheless, the water content needs to be controlled in testing environments especially where ionization due to the discharge is anticipated. Water vapor can

undergo dissociation and alter in this way the testing atmosphere to a great extent.

Testing at two different pressure levels in helium and in oxygen showed very interesting results, Fig. 6. The fatigue life in oxygen at a pressure of 0.1 torr was increased with respect to that at a pressure of 45 torr. The increase from 1.3 to 3.1 million cycles is in a good agreement with observations of other authors (6) for copper in reversed bending. Similarly, the fatigue life in helium at the identical pressures was increased from 5.9 to about 14 million cycles. The change in fatigue life in both gases was proportional since the ratios of fatigue life at low pressure to fatigue life at higher pressure were found to be approximately 2.4 for both the oxygen and the helium.

3.2 Effect of Irradiation

Irradiation of the specimen by electrons or ions caused in many instances a further reduction of the fatigue life compared to the number of cycles in the same gas without irradiation. To facilitate the discussion of the data on irradiation, the results were plotted in the bar graph shown in Fig. 8. The additional reduction of the fatigue life was found very small in oxygen. There was no distinct difference whether the specimen was negative i.e. received irradiation by oxygen ions or positive i.e. was a subject to electron impact.

Unlike in oxygen, the fatigue life in nitrogen under irrad-

iation showed a dependence on polarization causing more reduction in the number of cycles to failure for positive (electron) irradiation and less for the negative one. The irradiation by electrons reduced the fatigue life to the same life as that in oxygen.

Similarly in argon the electron irradiation was found more effective in reducing the fatigue life than irradiation by ions. The latter however, resulted in only a very small reduction with respect to the number of cycles in argon without irradiation.

A rather different effect of irradiation was observed in case of hydrogen. Both the electron and the ion irradiation caused a substantial increase of the fatigue life. Thus, irradiation in hydrogen increases the fatigue life beyond that obtained in argon atmosphere. The observed increase was found to be independent on the type of irradiation since the fatigue life was within the same range for both the irradiation by ions and by electrons.

Regardless of the environment a coating was formed on the specimen surface when the specimen was subjected to electron impact. This was also observed by other investigators (24). In case of reversed polarity a similar coating was formed on the electrode opposite the test specimen. An X-ray diffraction analysis of one of the coatings formed in hydrogen atmosphere showed that Cu_2O, CuO, $6CuO.Cu_2O$ were present. However, it is suspected that a complex noncrystalline compound is formed. The effect of ionization is usually accompanied by the deposition of foreign material. This contamination can be explained by the adsorption of residual

impurities, namely carbon or other organic molecules present in the apparatus and having undergone dissociation and polymerization due to collisions with the ion beam. Since the coatings (black in color) look alike in all gases, it is believed that they have the same origin such as traces of diffusion pump oil, vacuum grease, vapors from electrical wiring and insulation, rubber seals, impurities in the gases.

There was a definite removal of material from the surface due to sputtering when the specimen was irradiated by ions in any environment. From measurement of the weight loss and the thickness respectively, it was found that specimens irradiated by ions during fatiguing in hydrogen experienced a weight loss of 2×10^{-3}g. This measured weight loss corresponds to the removal of a layer 10^{-2}mm thick that is in order of 10^{5} atomic layers.

To investigate whether the effect of irradiation occurs only during the cycling, a few tests were performed where the specimen was irradiated by the discharge before fatiguing for a period of time corresponding to the fatigue life under irradiation in a given gas. One such test performed in oxygen with electron irradiation before testing resulted in practically the same fatigue life as the tests in oxygen without any irradiation (Fig. 5). This indicates that the black film has little effect, if any, on the fatigue life. Testing in hydrogen with irradiation before cycling gave rather contradictory results. Two specimens irradiated before testing by hydrogen ions showed absolutely different fatigue lives, one

being in the range of fatigue lives obtained in hydrogen without irradiation and the other far below (Fig. 5). Additional tests would be necessary to analyse the effect.

3.3 Effect of Ionic Bombardment

The difference in irradiation by the ion gun and by the glow discharge consists in the electrode processes. In the case of the glow discharge the specimen itself is the anode or the cathode. It means that the electrode processes take place right on the specimen surface. When the ion gun is used, the specimen is not a part of the circuit. It is merely a target. From exploratory tests with the ion gun, it was found that the ion beam produces a mild etching at grain boundaries at a distance of 1.5 inch between the gun and the test specimen. It was thought that the etching would speed up the fatigue process mainly by promoting the cracking due to preferential etching at grain boundaries and at slip bands. Result of one such test (Table 3) where the specimen was bombarded during fatiguing in oxygen showed no difference in fatigue life with respect to the fatigue life in oxygen at the pressure necessary for the formation of the ion beam. The surface of the specimen remained bright without any sign of oxide formation. This indicates that the etching caused by the ion gun at a distance of 1.5 inch does not influence the fatigue life of copper. This is in contrast with the irradiation by the glow discharge where the irradiation by ions in oxygen reduces the fatigue life and produces sputtering on the

surface.

3.4 Frequency Change During Fatigue Cycling

The recordings of frequency versus time are generally similar for all environments tested. The only significant difference is that they differ in length which represents the duration in each testing atmosphere. A typical frequency - time curve is presented in Fig. 9. After an initial period of strain hardening, a very gradual decrease of frequency is observed. The period of strain hardening itself is very short and sometimes is completed within the time spent by mounting the specimen, setting the contacts and balancing the vibrator.

The fatigue crack initiation cannot be readily detected on the recording. Metallographic observation showed slip bands cracking in oxygen and in helium after only a 6 per cent and 1 per cent of the total time to failure respectively. In most cases one cannot distinguish between the crack initiation and the stage I crack propagation from the shape of the curve. It is quite likely that the crack initiation is completed in the first few hundred cycles. Beachem (26) even found slip band cracking after only five cycles in tension - compression fatigue of iron.

The net decrease of the frequency that follows is of a straight line relationship and represents the stage I crack propagation. At about 300,000 cycles before failure regardless of the environment, the decrease is more and more pronounced, indicating that the stage

II crack propagation has begun. The shape of the curve is changed to a hyperbolic one. The fact that the last part of the curve (stage II crack propagation) occupies more or less the same time in any environment, even though slight differences in the shape exist, indicates that it is not the stage II crack propagation which is affected by the environment, rather it is the stage I of crack propagation that is influenced and is responsible for the observed differences in fatigue life.

3.5 Visible Light Fractography

Low magnification fractography shows that the fracture surfaces look similar in all environments tested. Fig. 10 shows a typical fracture surface produced in nitrogen. The fracture surfaces of specimens which were not irradiated during testing are bright and shiny. In case of irradiation the fracture surfaces are discolored to some extent.

The fracture surface of a specimen tested in oxygen under irradiation by ions exhibits many steps. The two crack fronts from opposite free surfaces propagated uniformly and joined approximately in the middle of the specimen cross-section. This indicates that conditions of plane strain were retained throughout the test. The uniform crack propagation was found in most tests in all environments. Some fine oxide inclusions are found to be dispersed throughout the fracture surface. These oxides may have been present in the material itself or were formed during the testing.

The fracture surface that was produced in oxygen under electron irradiation is basically the same. It is rough with the presence of oxides. The side which was close to the electrode shows penetration of oxide in form of a layer. The penetration goes to a depth of 9 per cent of the specimen thickness only. This shows that the irradiation by electrons is accompanied by an increased rate of chemical reactions.

When the specimen was irradiated by electrons in nitrogen an increased chemical activity was observed on the fracture surface. The surface was more attacked than in oxygen. This observation explains why the fatigue life was reduced in this case.

Irradiation by ions in nitrogen caused a discoloration of the fracture surface to a depth of 8 per cent which is less than in case of electron irradiation. The increased rate of reaction was probably minimized by the removal of a surface layer due to sputtering.

The presence of fine dispersed oxides on the fracture surface of the specimen tested in argon support the idea that the oxides were already present in the material. The fracture surface in argon is otherwise shiny, shows many crack initiation sites and a uniform advancement of the crack fronts from both sides.

Observation of the test specimen irradiated by hydrogen ions before testing shows no discoloration of any kind on the fracture surface. This is in contrast with irradiation by ions in hydrogen

during testing where the fracture surface was discolored to a very small extent. This confirms that the irradiation is only effective when done during the fatigue cycling.

3.6 Electron Fractography

Fatigue striations are a very typical feature of the fatigue fracture surface. Striations are curvilinear surface markings which resemble beach marks. They are, essentially, mutually parallel and at right angles to the local direction of crack propagation. In an ideal case, the striations are equal in number to the number of load cycles. Furthermore, the striations are generally grouped into patches and are bowed out in the direction of crack propagation. Striations are usually present in some proportions of most fatigue fracture surface areas in metals.

Observation of electron fractographs show that there is always a mixed mode of fracture present. The picture in Fig. 11 is a typical sample of the fracture surface of specimens tested in oxygen. One can observe fatigue striations which are not so clearly defined for copper as for aluminium and its alloys. The spacing of striations varies from one grain to another, however, it is uniform within one grain. The orientation of striations is different depending on the local direction of crack propagation. In addition to striations other interesting features can be seen. The presence of dimples is evident. This shows that separation also took place by tensile tear. The shape of dimples is elongated indicating that

the separation by tear was accompanied by an extensive shear deformation. In the right portion of Fig. 11 one can see so called stepwise crack growth. The stepwise growth can occur at low stress intensity levels.

Fig. 12 shows a feature that resembles serpentine glide in copper. However, a closer look shows fine striations on the fracture surface. This suggests that the serpentine glide-like appearance was formed by the rubbing of two mating surfaces after the crack had passed.

The micrograph in Fig. 13 gives an overall view of the fracture surface at lower magnification. It can be seen that some corrosion of the fracture surface has occured. Corrosion of the fracture surface is visible on the electron micrographs as black dots dispersed all over the area. The black dots are corrosion products which are sometimes transferred from the fracture surface on the replica during preparation. Depending on their size and orientation they appear black and sometimes cast white shadows. The overall fidelity of the replica is minimized because the corroded fracture surface looses its details. The fracture surface in Fig. 13 is rough. Fig. 14 shows an enlarged section with fatigue striations meeting a grain boundary. The striations are not the finest steps resolvable on the fracture surface. An enlarged section containing striations from Fig. 11 is shown in Fig. 15. One can clearly observe fine submarkings occuring between the striations.

The effect of irradiation did not bring a change in the overall appearance, however, an evidence of increased corrosion can be observed. The fractographs in Figs. 16 and 17 show fracture surfaces of specimens tested in oxygen under bombardment by ions and electrons respectively. The spacing between the striations seems to be wider than in the case of testing in oxygen without irradiation, thus indicating a more rapid crack propagation.

The fracture topographies of specimens tested in nitrogen atmosphere are somewhat different compared to those tested in oxygen. Fig. 18 gives an impression of a partially brittle fracture. This specimen was irradiated by ions. However, a look at the same picture at larger magnification, Fig. 19, reveals that the smooth faces are actually full of fine lines. It can be seen that stepwise growth took place (left bottom corner of Fig. 19) like in oxygen. On the right hand side one can see a kind of a river pattern which is very different from the river pattern observed in cleavage fracture. Dimples are not observed to a large extent. Fig. 20 shows again a fracture surface of a specimen tested in nitrogen under irradiation by ions. There is evidence of stepwise growth in this picture. In Fig. 21 which represents a specimen irradiated by electrons in nitrogen atmosphere basically the same features are observed as in Fig. 19 for ion bombardment. In addition, a few secondary cracks are formed within slip bands (right lower corner). The appearance of slip band cracks is explained later.

The fracture topography of specimens tested in an argon atmosphere is shown in Fig. 22. Again the appearance is almost like that of a brittle fracture. The facets appear to be smooth. Fatigue striations found in argon are poorly defined, Fig. 23. The presence of dimples in Fig. 22 suggests that separation accompanied by extensive shear took place. A surface feature termed stepwise growth (not shown) was part of the fracture topography as well. Part of the fracture surface was found to be corroded (Fig. 24). It is believed, however, that the corrosion either occured after the fatigue testing or the corrosion-like appearance was due to the contamination of the replica.

The fracture surface of a specimen tested in hydrogen atmosphere is shown in Fig. 25. Part of it looks like an intergranular brittle fracture. One can resolve, however, a substructure on the comparatively smooth facets. Fig. 26 gives evidence of intergranular brittle fracture where some grain faces are free of substructure. The right hand area of Fig. 26 and the bottom part of Fig. 25 show elongated dimples. The top part of Fig. 25 reveals the stepwise growth. In general, the fracture surface produced in hydrogen shows more brittle intergranular-like topography than any other environment. The fracture topography of specimens tested in humidified air looks more or less similar to that tested in hydrogen (Fig. 27). This suggests that hydrogen and water vapor act in a similar way.

The appearance of the fracture produced in helium can be seen in Fig. 28. This is the prevailing mode and is termed stepwise growth. The stepwise growth was found in any other environment but in no case in such a large proportion. Like in oxygen surface markings described as serpentine glide were found. They can be seen in Fig. 29. A question arises whether they represent true serpentine glide or were formed by rubbing action of two mating surfaces after the crack had passed. If the latter were true, they would be just deformed fatigue striations.

In general, striations which are typical for fatigue in other metals are not as distinct in reversed bending of copper.

3.7 Crack Initiation and Oxidation

A series of tests were performed in this project to study the effect of environment on crack nucleation. Two basically different environments were chosen, oxygen for its detrimental effect on the fatigue life, and helium because of its beneficial effect. Studies were conducted with the help of replication technique and transmission electron microscopy. The optical microscopy cannot be used for the determination of microcracks in the early stages of the fatigue process.

Cracks have to be of a comparatively large size to be detected by visible light microscopy. An example of a crack in a slip band as it appears in visible light is shown among optical micrographs later on (Fig. 40). The replication technique, however,

reveals surface cracks even of submicroscopic size. They become visible due to the penetration of the replicating tape into the submicrocracks (27). Even though tongues formed this way are partially torn or otherwise damaged during stripping of the tape, their debris, if favorably oriented, casts distinct shadows during the deposition of the shadowing metal. The submicrocracks are then easily recognized on the micrograph because the tongues (usually folded) appear black and cast white shadows.

The appearance of the free surface after fatiguing to failure in both helium and oxygen is shown in the micrographs in Figs. 30, 31. There is no basic difference between them. Perhaps the slip bands are more dense in helium than oxygen. This of course does not provide any indication of crack initiation. Therefore, two specimens were fatigued in oxygen for a limited time representing only a fraction of the total fatigue life. In the first case, the time of fatiguing was 6 hours (11 per cent of total fatigue life). Fig. 32 shows the slip pattern after 6 hours fatiguing and one can clearly see that slip band cracks are already well developed. It was decided to shorten the testing time to 3 hours. The deformation by slip on the free surface after 3 hours can be seen in Fig. 33. It is evident that slip band cracks are present even after only 6 per cent of the total fatigue life in oxygen. This of course suggests that the crack initiation period is completed very early at least in the oxygen atmosphere.

To clarify the effect of an inert environment, a test in

helium atmosphere was interrupted after 3 hours (1 per cent of total fatigue life) and investigated. The results are shown in Figs. 34 and 35. These electromicrographs were taken from different areas of the test section. Like in oxygen after 3 hours the slip band cracking can be resolved in both photographs with certainty. This observation means that the crack initiation period in helium is very short and is completed very early after only a small fraction of total number of cycles to failure. Since slip band cracks are found in both helium and oxygen atmospheres very early, it is concluded that the fatigue crack initiation is very little, if at all, influenced by the environment.

Close examination of the micrographs, Fig. 33, 34, 35, reveals dense, very fine, nearly parallel lines. Slip bands usually (but not always) run parallel with this fine substructure. They were found on the free surface of the specimen regardless of the environment. They were easily resolved in the optical microscope too. A replica of the free surface of the specimen was taken immediately after polishing. The specimen was not a subject of any deformation. Observation of the replica showed that the mentioned substructure was already present. The electron micrograph in Fig. 36 shows the unfatigued surface with the fine dense lines. It is likely that the fine structure is formed during the cooling period which followed after annealing as a consequence of thermal stresses. One can find a similarity between this substructure and the fine lines observed on the otherwise smooth facets on the fracture surface (Fig. 25).

The effect of ion bombardment on the surface was investigated with the help of electron microscopy as well. The electron micrograph, Fig. 37, shows the surface damage produced by ion irradiation in argon. Although the specimen was fatigued to failure and the area shown is in the vicinity of the main crack, no slip bands are observed. This fact indicates that the slip band bearing surface layer must have been removed by the irradiation. It is interesting that the cell structure shown in Fig. 37 was also found on the surface of an unfatigued specimen subjected to ion bombardment. The uniform cell structure is disturbed by the presence of a large rosette type oxide which is seen near the top right corner. The rosette type oxide is bluish in color and is shown at lower mganification later on in this thesis, in a color micrograph, Fig. 44. In addition to the cells and the large oxide one finds many dark dots with light shadows. It indicates that the dots were elevations at the time of deposition of shadowing material. Therefore, they must have been depressions in the surface of the specimen. They appear to be distributed randomly in quite a range of sizes.

A somewhat different form of damage to the fatigued surface was caused by ion bombardment in nitrogen. From Fig. 38 it can be seen that the irradiated surface retained a background which is characterized by the grain size and slip deformation. This suggests that the surface damage caused by nitrogen ions is milder than that caused by argon ions; the former producing a partial erosion of the deformation structure, the latter producing a complete

removal of the deformed surface layer. Like in argon, one can see the randomly distributed pits (Fig. 38).

As will be described further, bombardment by oxygen ions caused an erosion of the surface as well. For the sake of clarity, color photographs are used. They permit a distinct determination of the oxide distribution on the surface. The photomicrograph of Fig. 39 shows a free surface of a specimen bombarded by ions in an oxygen atmosphere. One can clearly see preferential oxidation within the slip bands. Areas between the slip bands remain free of oxidation. In the middle of Fig. 39 there is a crack running along the band causing oxide cracking. Unlike in argon, oxygen ion bombardment does not remove the slip pattern completely. Fig. 40 shows for comparison the surface of the same specimen which was not subjected to bombardment. The slip pattern typical of deformation by fatigue does not vary much with the environment. A crack can be seen in Fig. 40 which runs along the slip band. The surface was not oxidized. For this reason no color print was used. Cracking along slip bands was complemented by cracking along grain boundaries regardless of the environment. There are two kinds of oxides observed on the surface bombarded by oxygen ions. Both can be seen in Fig. 41. The first type is deposited in the slip bands, thus forming strips of oxides. They can be observed in the bottom part of the micrograph and in the top part where oxidation followed a cross-slip pattern. This kind of oxide appears in the early stages of fatigue testing. As the number of fatigue cycles

increases, some oxides strips grow and eventually join the neighboring strip forming that way an oxide layer. This is shown in the left bottom portion of Fig. 41. It is believed that they originate from oxide inclusions; and they are very often found cracked. The rosette type oxides become apparent in the later stages of fatiguing. A well developed oxide rosette is seen in Fig. 42 showing three superimposed layers of growth. Fig. 43 again shows the preferential oxidation in the slip bands and the oxide rosettes which appear to be cracked.

Argon ion irradiation also produces an oxide rosette structure probably due to the residual oxygen in the gas, Fig. 44. No slip band oxidation is visible.

4. DISCUSSION AND ANALYSIS

The experimental results confirmed that fatigue of copper is sensitive to gaseous environment. There are several ways in which the gaseous environment can be effective. These were reviewed by Westwood (19) and include: (1) adsorption; (2) interaction with the solid to produce a brittle surface compound, for example, an oxide; (3) by diffusion into the surface layers to produce a case-hardened layer; (4) by diffusion into the bulk followed by segregation at dislocations producing brittle behavior; (5) by bulk-diffusion followed by reaction to produce a hard and embrittling second phase; (6) by bulk diffusion followed by segregation or precipitation in voids or at precipitate particles.

It is likely that only the first two ways of interaction between the environment and the metal take place during fatiguing without irradiation.

4.1 Fatigue Crack Initiation

From the results of tests in this project it was concluded that crack initiation is practically not influenced by the environment. In copper fatigue crack nucleation occurs at the surface in zones of concentrated plastic flow. These zones are the surface slip bands. During the course of fatigue fine slip develops first probably by the operation of surface dislocation sources, or sources very close to the surface. The formation of slip bands that

follows usually occurs after fine slip has covered the entire surface of a crystal. The plastic deformation is then restricted to these bands. Plastic displacements within the slip band alter the surface topography. Displacements of opposite sign accumulate and form both intrusions and extrusions. The intrusions act as sharp notches causing a local rise in stress; they are nuclei of fatigue cracks.

To determine the effect of environment on crack nucleation a few short time tests were performed in oxygen and in helium. Results showed that slip band cracks were present on the free surface of specimens tested in oxygen for only three hours representing 6 per cent of cycles to failure (Fig. 33). Similarly a specimen tested in helium for three hours (1 per cent of cycles to failure) exhibited well developed cracks within slip bands (Fig. 35). This fact suggests that the effect of environment is very small, if it occurs at all. There may have been an effect within the period of three hours itself. Since the cracks were present already after a period of cycling representing only a small fraction of total fatigue life the possible differences in crack nucleation within the first three hours could not be responsible for such large differences in fatigue life which were exhibited. These observations are in a general agreement with Achter (18) who concludes that the major effect of the environment is on the rate of crack propagation.

The reason for the small effect of the gas environment on

crack nucleation seems to be the rate of the process in comparison with the rate of chemical interaction. The surfaces of the test specimens are always covered by a thin layer of oxide and by an adsorbed gas layer no matter how carefully they are handled. If the crack initiation rate is very fast the cracks can be nucleated before the oxygen from the adsorbed layer is used up and the surface can interact with the environment. In fact, as was mentioned earlier, Beachem (26) found slip band cracking after only five cycles in iron.

4.2 Fatigue Crack Propagation

The influence of environment on fatigue crack propagation is widely recognized. There are, however, two stages of crack propagation. The first stage is characterized by propagation of the crack on planes oriented at approximately 45 degrees to the stress axis. The crack propagation in stage II takes place on a plane perpendicular to the stress axis. The fracture surface in stage II is usually covered by striations running parallel to the crack propagating front. In the present case of lower strain fatigue and plane strain crack propagation most of the fatigue life is spent in stage I. Stage II, however, also plays an important part since this process actually fractures a large portion of the cross section of the specimen.

One of the proposed mechanisms of crack propagation in stage II is called plastic blunting process as outlined by Laird (28).

When the tensile load is applied the small double notch at the crack tip serves to concentrate slip zones along planes at 45 degrees to the plane of the crack and to maintain a square geometry of the tip. When the specimen is deformed to the maximum tensile strain the stress concentration of the crack is lessened, the slip zones at the tip broaden and the crack tip blunts to a semicircular configuration. Upon application of a compressional load the slip direction in the zones is reversed, the crack faces are crushed together and the new crack created in tension is forced into the plane of the crack and partly folded by buckling of the very front of the tip into another notch.

It is believed that the mechanism of stage I crack propagation is basically the same as that of stage II (28). In contrast to the stage II cracks propagate along the common slip planes and therefore at 45 degrees to the stress axis. The increase in crack length per cycle is accomplished by spreading of the crack tip to the width of the slip zone.

The plastic blunting theory was recently criticized by Pelloux (9). His argument is that the plastic blunting theory cannot explain the fracture surface reported recently by Meyn (29) who found absence of striations on the fracture surface on an aluminium alloy when tested in vacuum. Pelloux suggests a different model for fatigue crack propagation (Fig. 45). Deformation at the tip of a sharp notch can take place only by shear on two planes at 45 degrees to the plane of the crack. Deformation can proceed

either alternately on one band and then on the other or simultaneously. This process of deformation by alternating shear results in an extension of the notch by a mechanism of rupture and not by fracture. The sliding leads to the formation of a 90 degree notch tip which remains always sharp regardless of the magnitude of the alternating shear displacement. The process should be theoretically reversible. However, in practice the freshly exposed crack surface for most metals is immediately oxidized limiting so the amount of reversibility. The amount of reversible slip would reflect the aggressivity of the environment in this fashion. This model seems to be quite reasonable and explains the environmental effects satisfactorily.

It was concluded in the section on test results that stage I crack propagation is affected most extensively by the environment. Furthermore, oxygen was found to be the most damaging element in a sense of reduction of the fatigue life and thus reduction of stage I crack propagation. The conclusion regarding the effect of oxygen is based on the following observation.

There is evidence for residual content of oxygen in the gases used in this project (Table 2). Additional traces of oxygen may have come from the testing apparatus. The fatigue life of copper was increased in the sequence of oxygen, hydrogen, nitrogen, argon and helium (Fig. 5). This compares with the sequence of decrease in content of residual oxygen (Table 2). This suggests that oxygen is the determining factor in the environment. In an ideal

case of gases absolutely free of oxygen the fatigue lives should be governed only by adsorption of the gases to the surface and by its rate. The content of oxygen present as impurity decreases proportionally with the reduction in pressure. Support for this view is provided by the results of testing at two different pressure levels. The fatigue life of copper in helium was increased by a factor of 2.42 when the testing pressure was decreased from 45 torr to 0.1 torr. The same decrease in pressure of oxygen exhibited an increase in fatigue life by a factor of 2.44. The observed proportionality is remarkable.

A recent investigation by Smith and Shahinian (21) points out the importance of residual oxygen. They found an extreme sensitivity of nickel to the residual content of oxygen in the atmosphere which can lead to misinterpretation of the environmental effects. Smith et al. report a critical pressure of oxygen of 10^{-4} torr above which the fatigue life of nickel is drastically reduced. From this the authors conclude that the partial pressure of oxygen of 10^{-4} torr in the environment is capable of overriding the effect of the environment. Similar low critical pressures were found for the fatigue life of stainless steel in oxygen (18), and for lead (20) and aluminium (11) in air.

The sensitivity of copper to oxygen is not so pronounced. The fatigue life of copper in reversed bending as a function of air pressure shows a straight line relationship on a logarithmic scale (6). With respect to oxygen, a plot of the fatigue life of

copper versus oxygen pressure results in a mild curve (13) without any critical pressure at which a sudden change occurs. Testing at two different pressures of oxygen resulted in fatigue lives which are in close agreement with relationships just mentioned and shown in Fig. 46. The original diagram was obtained by Wadsworth and Hutchings (6) for O.F.H.C. copper in air. Comparison of the data procured in this project is made on the basis of partial pressure of oxygen. The higher fatigue lives obtained in this project are accounted for by the different configuration of the test specimen. Nevertheless, the straight line relationship holds. Therefore the residual content of oxygen cannot cause such striking differences in the fatigue life as it does in the case of nickel. However, the dependence of the fatigue life of copper on the oxygen lends additional support to the interpretation of sequence of gases versus the fatigue life.

4.3 Mechanisms of the Effect of Oxygen

As far as the mechanisms of the effect of oxygen is concerned the author believes that the rewelding theory in conjunction with the brittle film hypothesis can most satisfactorily explain the experimental observations. Testing in oxygen under ion irradiation indirectly supports this view. Increased reactivity of oxygen under discharge was indicated by the observation of increased oxidation. As discussed previously, preferred oxidation took place within slip bands (Figs. 39, 41, 43). This means that oxygen is

attracted by freshly created surfaces within the slip bands. It is most likely that oxygen also penetrates into the slip band cracks forming there an oxide layer on the new surfaces produced by crack extension; thus, preventing the rewelding of the crack surfaces during the compressive part of the cycle. It is believed that the presence of the oxide film has an additional important effect on the crack propagation. It further promotes crack propagation in accordance with the brittle film hypothesis. As illustrated in Fig. 47, the brittle oxide film at the crack tip can be easily ruptured during the tensile part of the cycle causing local stress concentration which reduces the required plastic deformation and makes the crack propagation easier. The brittle film hypothesis might explain the absence of the critical pressure for copper (see introduction).

4.4 Processes During Irradiation

The effect of irradiation by gaseous ions or electrons is rather complex. In oxygen, nitrogen and argon the irradiation enhances the effect of the gases which is reflected by an additional reduction of the fatigue life. In case of hydrogen the reverse is true and the fatigue life under irradiation was substantially increased.

There may be three possible ways of interaction between the specimen and the environment under irradiation: (1) removal of a layer; (2) formation of a layer; (3) diffusion of gas into the

solid. These three possibilities are in addition to oxidation which always takes place provided that oxygen is present. The rate of oxidation in ionized gases is believed to be increased mainly due to formation of monoatomic oxygen and ozone. In a glow discharge the following reactions can occur:

$$O_2 \longrightarrow O + O; \qquad O + O_2 \longrightarrow O_3$$

Ozone is known to be very reactive. Since the beam was focused well at the test section of the specimen, ozone being formed was available at the surfaces newly formed by plastic deformation. The amount of reversion was likely reduced due to the close proximity of the electrode processes at the specimen surface. The residual content of oxygen in the environment was probably increased due to decomposition of water vapor, electrical wiring, possible traces of diffusion pump oil and vacuum grease. There are several other reactions possible in addition to the formation of ozone. The presence of ozone seems to be the most important factor in case of oxygen, and the residual oxygen content in nitrogen and argon.

There is an effect of polarity, too. When the specimen is made a cathode and receives bombardment by ions it suffers a damage known as cathodic sputtering. The rate of sputtering is a function of the nature of the ion beam i.e. the number of atoms removed per unit time varies directly as the atomic number of the ions (24). This dependence could be clearly observed on the surfaces of fatigue specimens subjected to irradiation by ions. The largest damage was observed in case of argon when the slip

markings on the surface were completely removed (Fig. 37). Specimens irradiated by oxygen ions showed some slip bands with preferential oxidation (Fig. 41). In case of nitrogen remnants of the slip pattern were retained (Fig. 38). There was, of course, a difference in irradiation time which was identical with the fatigue life. Data available in the literature on sputtering yield support to the differences in the surface appearance which was observed. The sputtering yield for argon (high atomic number) was twice of that for nitrogen (low atomic number) as quoted by Carter (30).

Another phenomenon which occurs in the course of bombardment is the introduction of gases into the solid. It is possible with the energies used in this project to inject gas atoms into the metal to a depth of several tens of microns (31). This mechanism is competing with sputtering.

One other effect of bombardment is the introduction of lattice defects. According to Carter (32) the threshold energy for a copper atom to be displaced from its equilibrium position is 25 ev. This energy can be transferred to a copper atom by a proton having an energy of 410 ev. This compares with 450 ev used in this project. It appears that introduction of lattice defects was not significant due to the comparatively low energy used.

When the polarity was reversed and the specimen made the anode it received irradiation by electrons. In addition a black coating was always formed with this set up. This is commonly observed in vacua of less than 10^{-9} torr. In the case of the oxygen atmos-

phere there was no difference in fatigue life with respect to the bombardment by ions or by electrons. The effect on the fatigue life was mainly due to rapid oxidation rather than to irradiation. In case of nitrogen and argon the fatigue life of specimens irradiated by electrons was found to be shorter with respect to irradiation by ions for these gases. The presence of the coating on the specimen surface was probably acting as a brittle film, thus promoting cracking.

The behavior in hydrogen under irradiation is very different from that in the other gas environments. Both polarities caused a considerable increase of the fatigue life of copper. This could be due to some strengthening mechanism. The possible interaction may involve diffusion of monoatomic hydrogen into the lattice and interaction with dislocations or stacking faults. This in turn would influence the dislocations activities at the surface by making cross-slip and jogging of screw dislocations more difficult. Consequently formation and growth of cracks would be delayed.

The amount of cross-slip in specimens irradiated by ions or electrons in hydrogen was not reduced, however. Therefore the mechanism of strengthening outlined above seems to be improbable. A more real explanation of the effect of hydrogen under irradiation suggests that a chemical reaction took place. Monoatomic hydrogen can react with residual oxygen in the environment and form water vapor. The observed increase in fatigue life would be then a consequence of a reduction of residual oxygen in the atmosphere.

The increase of water vapor content does not have an effect in the absence of oxygen (6). If there is a detrimental effect of water vapor it will be overcome by a stronger effect due to the removal of oxygen according to the reaction:

$$2H^{+} + O^{-} \longrightarrow H_2O$$

4.5 Free Surface Characteristics

The cell structure present on the surface of specimens irradiated by argon ions (Fig. 37) is similar to a dislocation cell structure observed with thin foils electron microscopy. There is a dimensional disagreement, however. Feltner and Laird (33) working with copper presented a series of micrographs with the cell size of approximately 0.5 microns. The size of the cells depends on the magnitude of cyclic strain and the tests temperature to some extent. The size of the cells in the cell-like structure obtained in argon is an order of magnitude larger than that observed by other authors. The cell-like structure of the same size was produced by ion irradiation without fatiguing and even without chemical polishing. This suggests that the cells formed were neither a consequence of fatiguing nor of chemical polishing.

The fine dense lines observed on the free surface of the unfatigued specimen (Fig. 36) are believed to be fine slip lines. Their spacing is approximately 700 Å which is in the range from 300 Å to 800 Å quoted by Grosskreutz and Benson (34) for fine slip. The fine slip may have been formed during the cooling period

that follows after annealing due to thermal stresses caused by thermal and elastic anisotropy in the specimen.

4.6 Fracture Topography

The fracture topography reflects to some extent the environment. The comparatively large proportion of striations on the fracture surface produced in oxygen (Fig. 11) confirms that oxygen makes crack propagation easier. The elongated dimples which were found to some extent on the fracture surfaces produced in any environments are accounted for by two different mechanisms. Since the fatigue crack growth in polycrystalline materials is selective cracks advance by regular crystalographic processes in favorably oriented grains. This process is characterized by striations. On the other hand, grains which are not favorably oriented are ruptured by ductile tearing (35). This mechanism seems to be responsible for most of the dimples observed on the fracture surface.

The other mechanism explains dimples as a consequence of ductile tearing connecting different levels of crack propagation (1). This mechanism did not play an important part in this project because the areas containing dimples were corresponding to the grain size.

The intergranular separation as it appears for example, in Fig. 19, seems to be typical for fractures in copper. Hoeppner (36) who studied the effect of grain size on crack propagation in copper presented a few micrographs showing crystalline facets similar to

those shown in Fig. 19. He suggests that the facetted appearance is a result of crack propagation between grain, twin, and sub-boundaries. The facets usually contain slip lines formed after the surfaces have parted. They should not be confused with striations. Slip lines sometimes appear between striations as a substructure.

The effect of the environment on the fracture topography can be summarized as follows:

The fracture surface contains striations, dimples, facets and stepwise growth in all environments. Striations which are found in largest proportions in oxygen are replaced in other environments to some extent by other features namely by brittle fracture appearance and stepwise growth. Furthermore, the striations are poorly defined in inert environments. This observation supports the crack propagation mechanism proposed by Pelloux (9).

5. SUMMARY AND CONCLUSIONS

1. The fatigue life of O.F.H.C. copper in different gases at reduced pressure increases in the sequence oxygen, hydrogen, nitrogen, argon, helium. Relative to oxygen the maximum increase in helium was by a factor of 4. The fatigue lives are directly related to the residual oxygen content of the various gases.
2. The difference in fatigue life are related to the stage I of fatigue crack propagation since the stage II crack propagation requires the same number of cycles regardless of the environment.
3. Crack initiation takes place very early during the fatigue life. Electron microscopy showed slip band cracking to occur at about 6 per cent and 1 per cent of the total time to failure in oxygen and helium respectively.
4. The effect of water vapor is not very pronounced because testing in dessicated air and humidified air (96 per cent relative humidity) caused a difference in fatigue life that was less than 10 per cent. However, reduction of the oxygen pressure from 45 torr to 0.1 torr produced an increase in the fatigue life by a factor of 2.4. This suggests oxygen is by far the more damaging element than water vapor.
5. Testing at different pressure levels in oxygen shows that reduction of oxygen pressure yields an increase in fatigue life that is in good agreement with observations reported

by other investigators.

6. Irradiation of the specimen surface with gas ions or electrons causes a further reduction of the fatigue life except for hydrogen gas where the reverse is true.
7. The behavior in hydrogen is believed to be related to the removal of residual oxygen by formation of water.
8. The residual content of oxygen in the system is probably increased by irradiation due to dissociation of water vapor, traces of diffusion pump oil etc. which seems to be responsible for the reduction of the fatigue life under irradiation for a given environment with exception of hydrogen.
9. The influence of irradiation combines an increased rate of reaction of the solid and the gas with a removal of the specimen surface layer due to collisions with gas ions.
10. Irradiation of the specimen by either ions or electrons with a potential drop of 450 v between the anode and cathode and a total current of 9 ma caused removal of a layer due to sputtering from the specimen surface when the specimen was irradiated by ions. Irradiation by electrons caused formation of a black coating on the specimen surface.
11. Bombardment of the specimen surface during fatiguing with a beam of ions produced by an ion gun having 2000 v difference between the anode and grounded cathode has no effect on the fatigue life of copper in oxygen. However, etching of the specimen surface is observed.

12. Difference in surface damage were found depending on whether the specimen was a target or one of the electrodes producing mild etching or heavy sputtering respectively.

13. Oxidation during cycling under irradiation by oxygen ions takes place by two mechanisms. In the early stages of fatigue preferred oxidation occurs within the slip bands. In later stages formation of rosette-type oxides is observed.

14. The testing temperature of the specimen under irradiation is not increased much due to the impact of electrons or ions as measured by a thermocouple embedded in a specially prepared specimen. The maximum operating temperature of 34°C was found for the test specimen being subject to ionic impact.

15. Fractographic analysis shows there is no difference in the fracture mode for different environments. A mixed inter-crystalline-transcrystalline mode of fracture was always found. However, the fracture topography reflects the effect of environment to some extent.

REFERENCES

1. Plumbridge, W.J., and Ryder, D.A., Metallurgical Reviews, 1969, Vol. 14, pp. 119-142.
2. Kramer, I.R., Fatigue-An Interdisciplinary Approach, Syracuse University Press, Syracuse, 1964, p. 245.
3. Bennet, J.A., Fatigue-An Interdisciplinary Approach, Syracuse University Press, Syracuse, 1964, p. 209.
4. Frost, N.E., Applied Materials Research, 1964, Vol. 3, No. 3, p. 131.
5. Broom, T., and Nicholson, A., Journal, Institute of Metals, 1961, Vo. 89, p. 183.
6. Wadsworth, N.J., and Hutchings, J., Phil Mag. 3, 1958, p. 1154.
7. Feeney, J.A. et al., Metallurgical Transactions, 1970, Vol. 1, No. 6, p. 1741.
8. Meyn, D.A., Transactions ASM, 1968, Vol. 61, p. 52.
9. Pelloux, R.M.N., Transactions ASM, 1969, Vol. 62, pp. 281-285.
10. Grosskreutz, J.C., and Bowles, C.Q., Environment-Sensitive Mechanical Behavior, Gordon and Breach, New York, 1966, p. 67.
11. Shen, H., Podlaseck, S.E., and Kramer, I.R., Acta Metallurgica, 1966, Vol. 14, p. 341.
12. Bradshaw, F.J., and Wheeler, C., Applied Materials Research, 1966, Vol. 5, No. 2, p. 112.

13. Achter, M.R., Danek, G.J.,Jr., and Smith, H.H., Transactions, AIME, 1963, Vol. 227, p. 1296.

14. Shives, T.R., and Bennet, J.A., Journal of Materials, 1968, Vol. 3, No. 3, pp. 695-715.

15. Laird, C., and Smith, G.L., Philosophical Magazine, 1963, Vol. 8, p. 1945.

16. Grosskreutz, J.C., quoted by Achter, M.R., ref. 2, p. 188.

17. Martin, D.E., Transactions, Am. Soc. Mechanical Engrs., 1965, Vol. 87, p. 850.

18. Achter, M.R., Fatigue Crack Propagation, ASTM STP 415, ASTM, 1967, p. 187.

19. Westwood, A.R.C., Environment-Sensitive Mechanical Behavior, Gordon and Breach, New York, 1966, p. 52.

20. Snowden, K.V., Acta Metallurgica, 1964, Vol. 12, p. 295.

21. Smith, H.H., and Shahinian, P., Effect of Environment and Complex Load History on Fatigue Life, ASTM STP 462, ASTM, 1970, pp. 217-232.

22. McTaggart, F.K., Plasma Chemistry in Electrical Discharges, Elsevier Publishing Company, Amsterdam, 1967, p. 126.

23. Siebel, E., and Staehli, G., Archiv fur das Eisenhuttenwesen, 1941/1942, Vol. 15, pp. 519-527.

24. Trillat, J.J., Ionic Bombardment Theory and Application, Gordon & Breach, New York, 1964, p. 19.

25. Vitovec, F.H., DRB Progress Report, October 1968.

26. Beachem, C.D., The Usefulness of Fractography, Paper No. 46, ASTM, 1967.

27. Beachem, C.D., Fracture, Vol. 1, Academic Press, Inc., New York, 1968, p. 243.

28. Laird, C., Fatigue Crack Propagation, p. 131, ASTM STP 415, ASTM, 1967.

29. Meyn, D.A., Transactions ASM, 1968, Vol. 61, p. 42.

30. Carter, G., and Colligon, J.S., Ion Bombardment of Solids, Heineman Educational Books Ltd., London, 1968, p. 325.

31. Brebec, G. et al., Ionic Bombardment Theory and Applications, Gordon & Breach, New York, 1964, p. 220.

32. Carter, G., and Colligon, J.S., Ion Bombardment of Solids, Heineman Educational Books Ltd., London, 1968, p. 214.

33. Feltner, C.E., and Laird, C., Acta Metallurgica,1967, Vol. 15, No. 10, p. 1633.

34. Grosskreutz, J.C., and Benson, D.K., Surfaces and Interfaces II, Syracuse University Press, Syracuse, 1968, p. 61.

35. Hertzberg, R.W., Fatigue Crack Propagation, ASTM STP 415, ASTM, 1967, p. 205.

36. Hoeppner, D.W., Fatigue Crack Propagation, ASTM STP 415, ASTM, 1967, p. 486.

TABLES

TABLE 1

Spectographic Analyses of OFHC Copper

Element	Concentration (ppm)	
	Specimen 1	Specimen 2
O_2	3	<3
Ag	10	10
Fe	1	1
S	9	12
As	<3	<3
Pb	7	6
P	<1	<1
Sb	4	4
Bi	0.2	0.2
Te	<2	<2
Sn	2	1
Zn	<0.5	<0.5
Ni	3	3
Hg	<1	<1
Cd	<0.1	<0.1
Mn	<0.1	<0.1
Conductivity (% IACS)	101.7	101.6
Bends*	12-11	12-11

* Represents number of 90° reverse bends before breaking of 0.080 in. dia. wire heated for 30 min. in hydrogen at 850°C and quenched.

TABLE 2

Specification of Impurities in Gases

Argon	99.996%	
Oxygen		1 PPM
Nitrogen		2 PPM
Hydrogen		1 PPM
Carbon Bearing Gas		2 PPM
Moisture		13 PPM
Helium	99.995%	
Oxygen		0.3 PPM
Nitrogen		1.2 PPM
Hydrogen		0.01 PPM
Neon		14.3 PPM
Hydrocarbons		0.05 PPM
Hydrogen	99.99%	Dew Point Less than -65 F
Oxygen		4 PPM Max.
Nitrogen	99.998%	
Oxygen		2 PPM
Argon		15 PPM
Hydrocarbons		1 PPM
Carbon dioxide		0.25 PPM
Moisture		2.5 PPM
Oxygen	99.6%	
Nitrogen		0.15%
Argon		0.25%
Carbon dioxide		5 PPM
Moisture		3 PPM

TABLE 3

Fatigue Test Data

Test Specimen No.	Atmosphere	Pressure (torr)	Irradiation	Average Frequency (Hz)	Cycles to Failure (10^6 cycles)	Strain Amplitude (10^{-6} in./in)	Calculated Stress (psi)
30	O_2	45		17.7	0.955	1820	18400
31	O_2	45		17.8	1.455	1820	18100
67	O_2	45		18.0	1.360	1850	18400
55	O_2	0.1		17.6	3.340	1850	18400
57	O_2	0.1		17.9	2.940	1890	18800
64	O_2	0.1	I.G.	17.3	1.960	1820	18100
43	O_2	45	+	18.4	0.875	1878	18700
45	O_2	45	+	17.8	1.280	1820	18100
27	O_2	45	-	18.4	0.812	1850	18400
29	O_2	45	-	18.1	0.826	1878	18700
65	O_2	45	-	17.2	0.960	1850	18400
66	O_2	45	-	17.2	1.240	1820	18100
47	O_2	45	+B.T.	18.8	1.520	1890	18800
32	N_2	45		17.8	1.635	1850	18400
33	N_2	45		17.7	1.620	1820	18100
28	N_2	45	+	16.8	1.285	1820	18100
34	N_2	45	+	16.5	0.946	1850	18400

TABLE 3 (cont'd)

Test Specimen No.	Atmosphere	Pressure (torr)	Irradiation	Average Frequency (Hz)	Cycles to Failure (10^6 cycles)	Strain Amplitude (10^{-6} in./in)	Calculated Stress (psi)
24	N_2	45	-	15.8	1.330	1788	17800
26	N_2	45	-	15.7	1.460	1758	17500
35	H_2	45		17.9	1.110	1850	18400
36	H_2	45		17.7	1.610	1820	18100
38	H_2	45	+	18.1	2.840	1905	19000
40	H_2	45	+	17.4	2.290	1850	18400
52	H_2	45	+B.T.	18.5	1.260	1820	18100
51	H_2	45	+B.T.	18.4	0.830	1850	18400
41	H_2	45	-	16.9	2.300	1850	18400
42	H_2	45	-	17.9	2.810	1878	18700
21	A	45		17.4	1.865	1820	18100
37	A	45		17.3	2.500	1820	18100
39	A	45		17.6	1.805	1820	18100
46	A	45		17.1	1.720	1936	19200
23	A	45	+	17.7	1.392	1878	18700
44	A	45	+	17.5	1.140	1820	18100
22	A	45	-	16.8	2.330	1820	18100
25	A	45	-	16.1	1.678	1936	19200

TABLE 3 (cont'd)

Test Specimen No.	Atmosphere	Pressure (torr)	Irradiation	Average Frequency (Hz)	Cycles to Failure (10^{-6} cycles)	Strain Amplitude (10^{-6} in./in)	Calculated Stress (psi)
68	He	45		18.4	5.920	1890	18800
53	He	0.1		17.6	15.200	1850	18400
58	He	0.1		17.3	14.300	1890	18800
60	He	0.1		16.7	13.600	1850	18400
48	dessicated air	atmospheric		17.9	1.950	1850	18400
49	humid air 96% r.h.	atmospheric		18.5	1.870	1850	18400
50	humid air 96% r.h.	atmospheric		17.6	1.750	18500	18400

I.G. bombardment by ion gun
\+ test specimen positive, irradiation by electrons
\- test specimen negative, irradiation by ions
B.T. irradiation before testing
% r.h. per cent relative humidity

FIGURES

FIG. 1 Fatigue test facility.

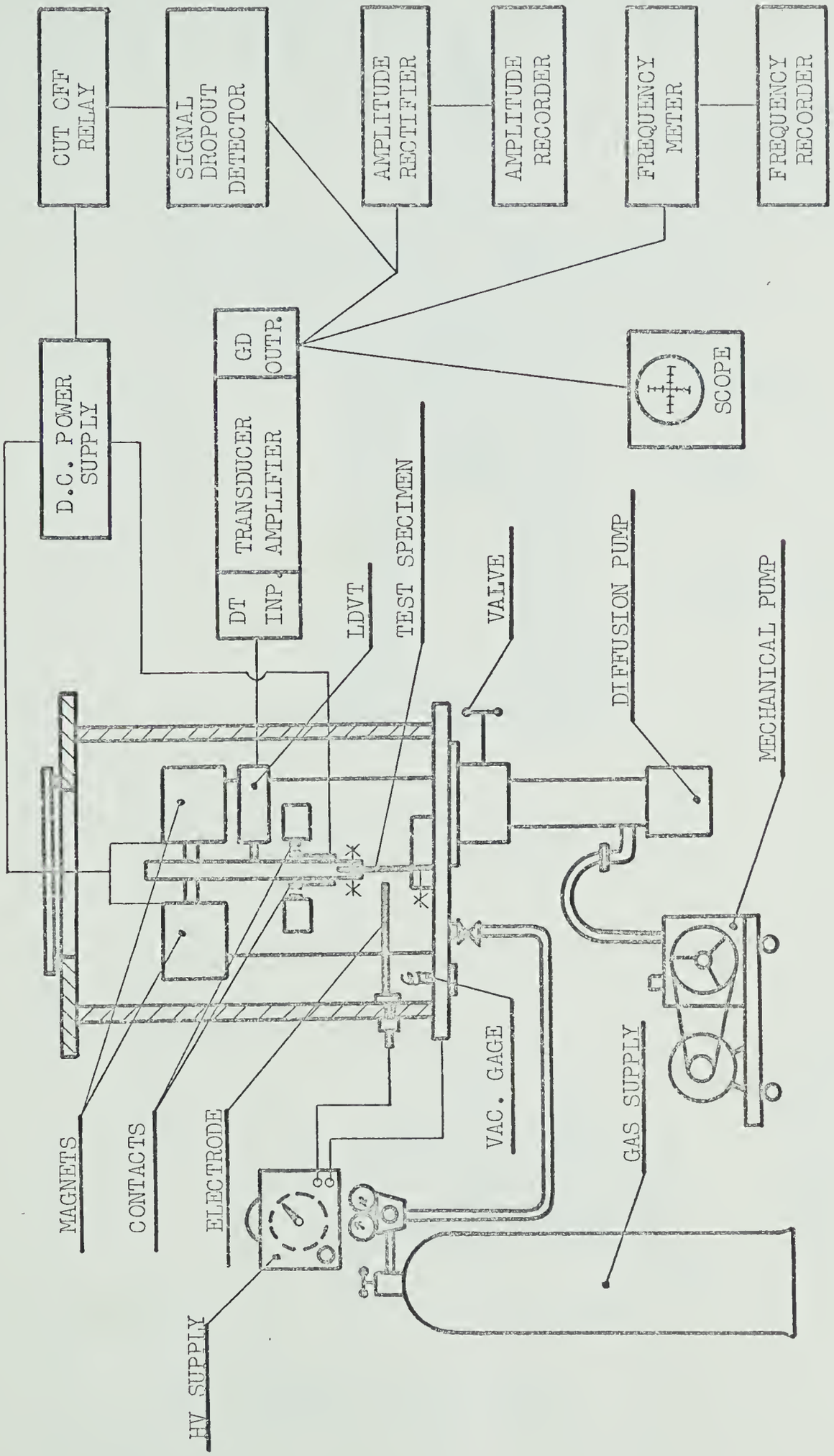

FIG. 2 Schematic diagram of test set-up.

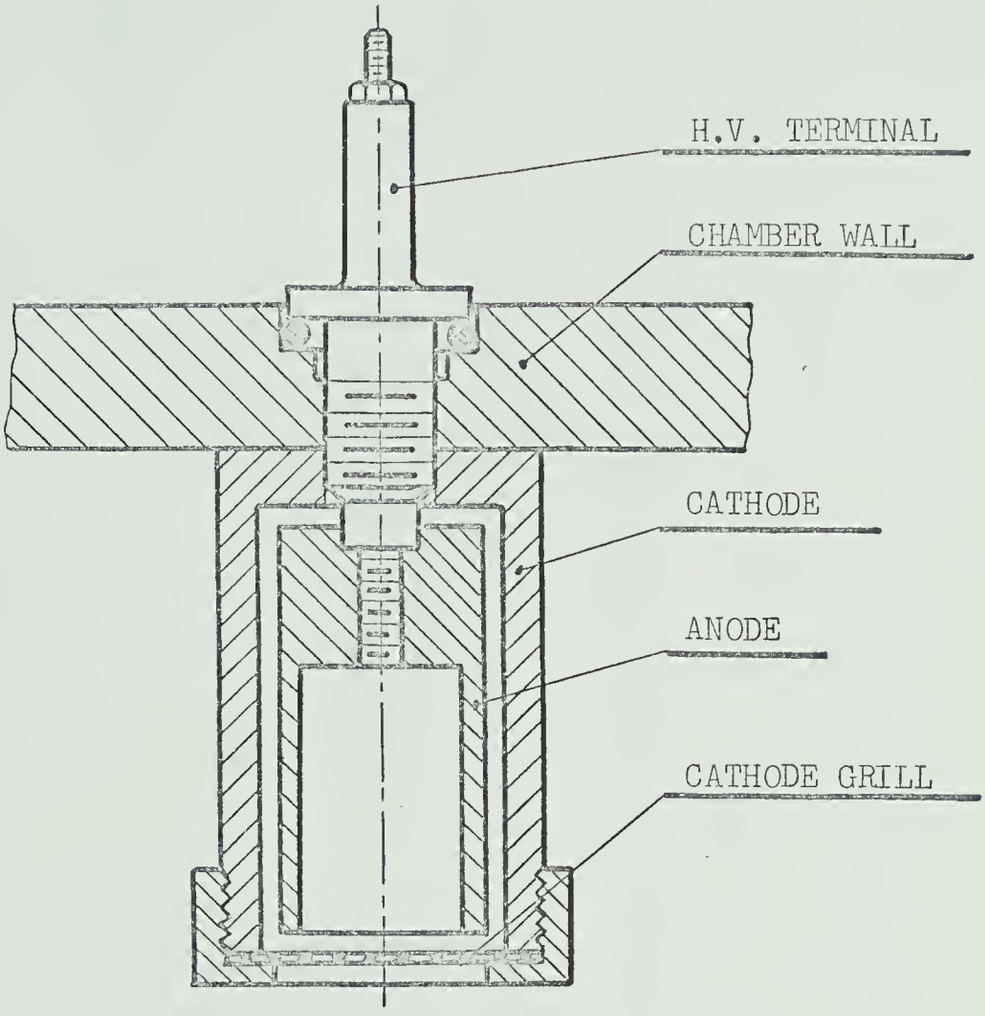

FIG. 3 Schematic diagram of the ion gun.
(Scale: 1 in. = 1 in.)

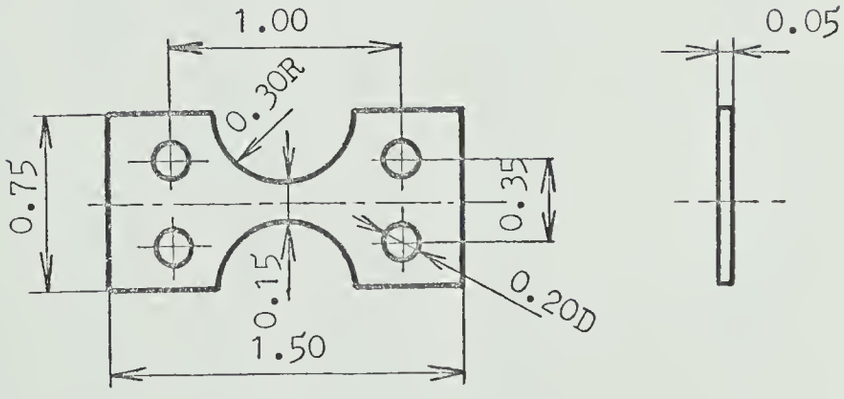

FIG. 4 Fatigue test specimen.
(Scale: 1 in. = 1 in.)

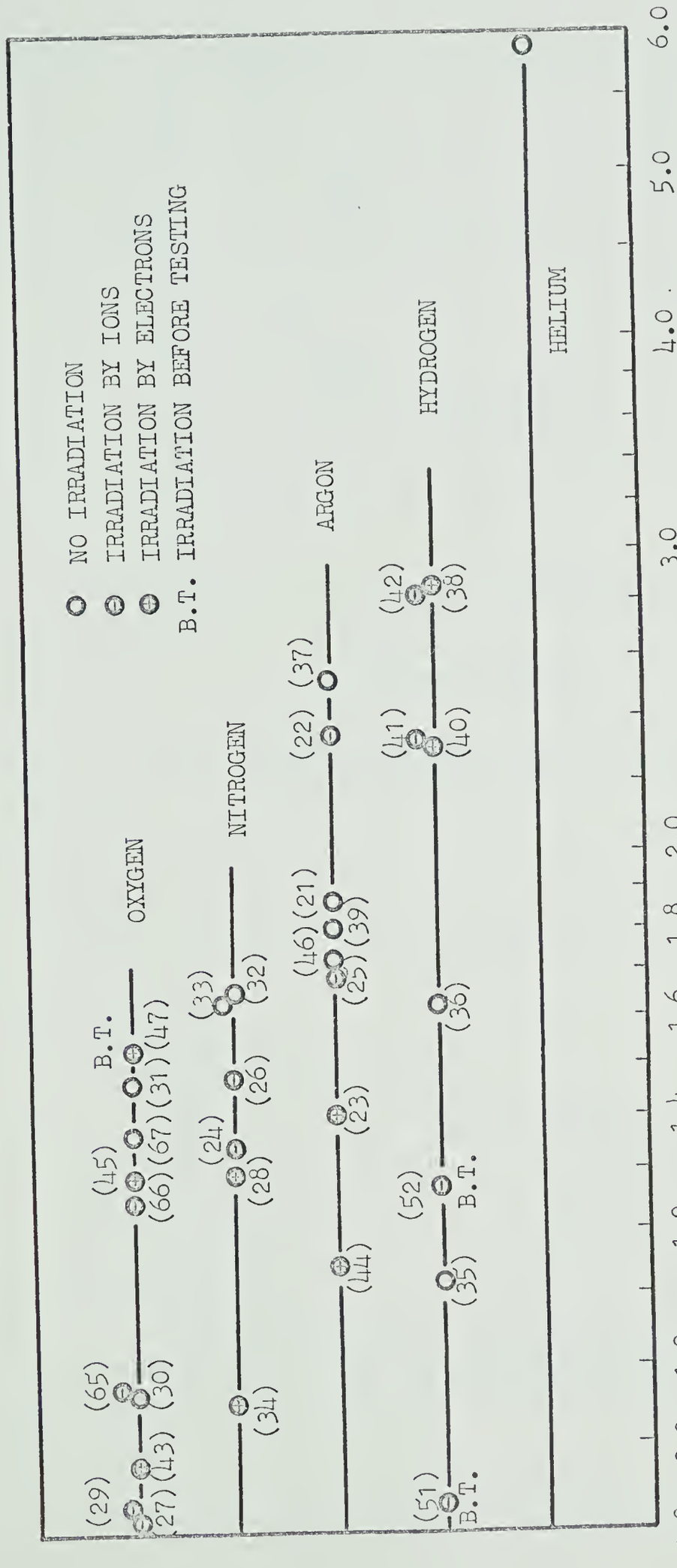

FIG. 5 Effect of environment on the number of cycles to failure.
Numbersin parentheses refer to the number of the test specimen.

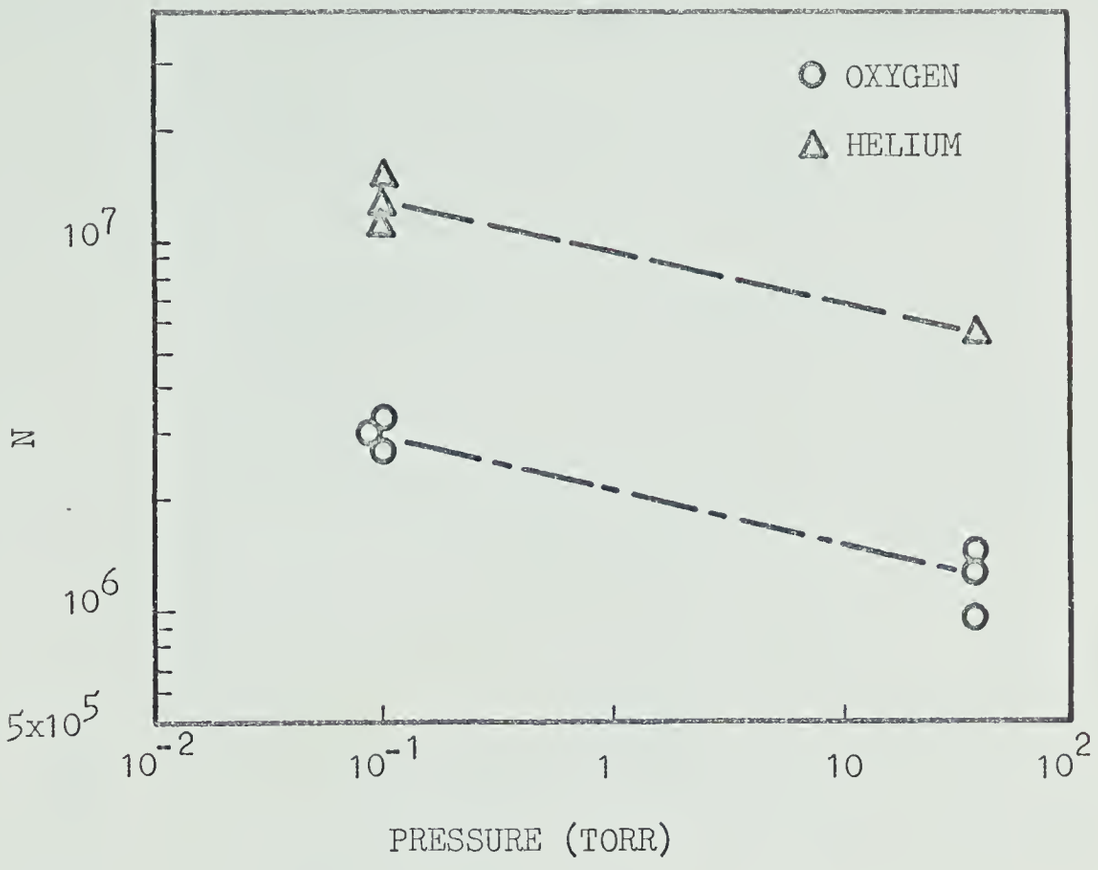

FIG. 6 Effect of pressure on the fatigue life.

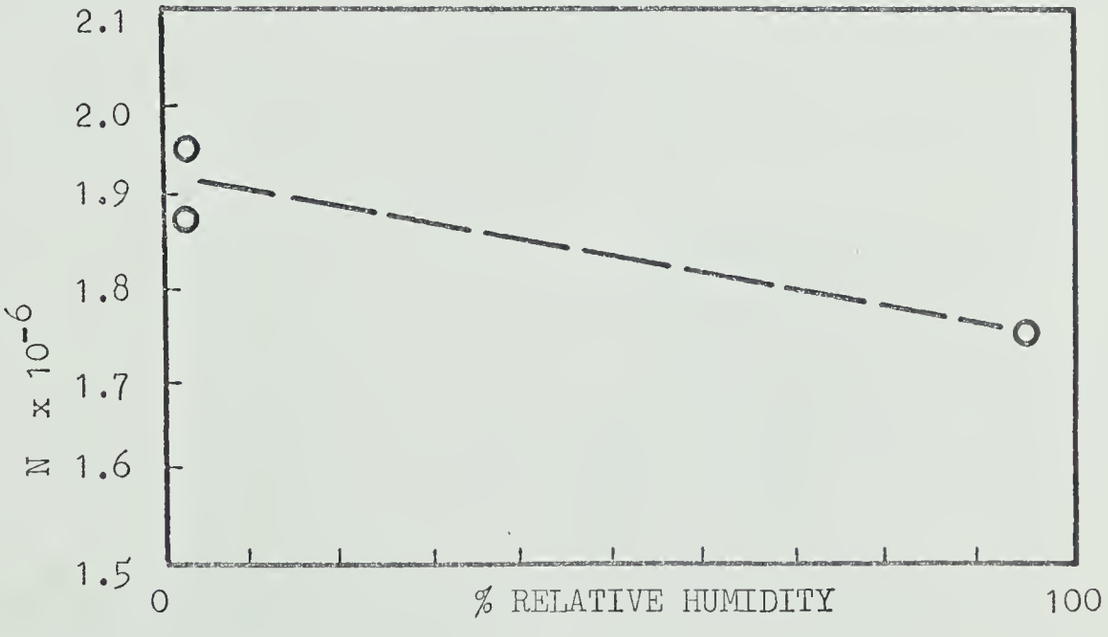

FIG. 7 Effect of moisture on the fatigue life in air.

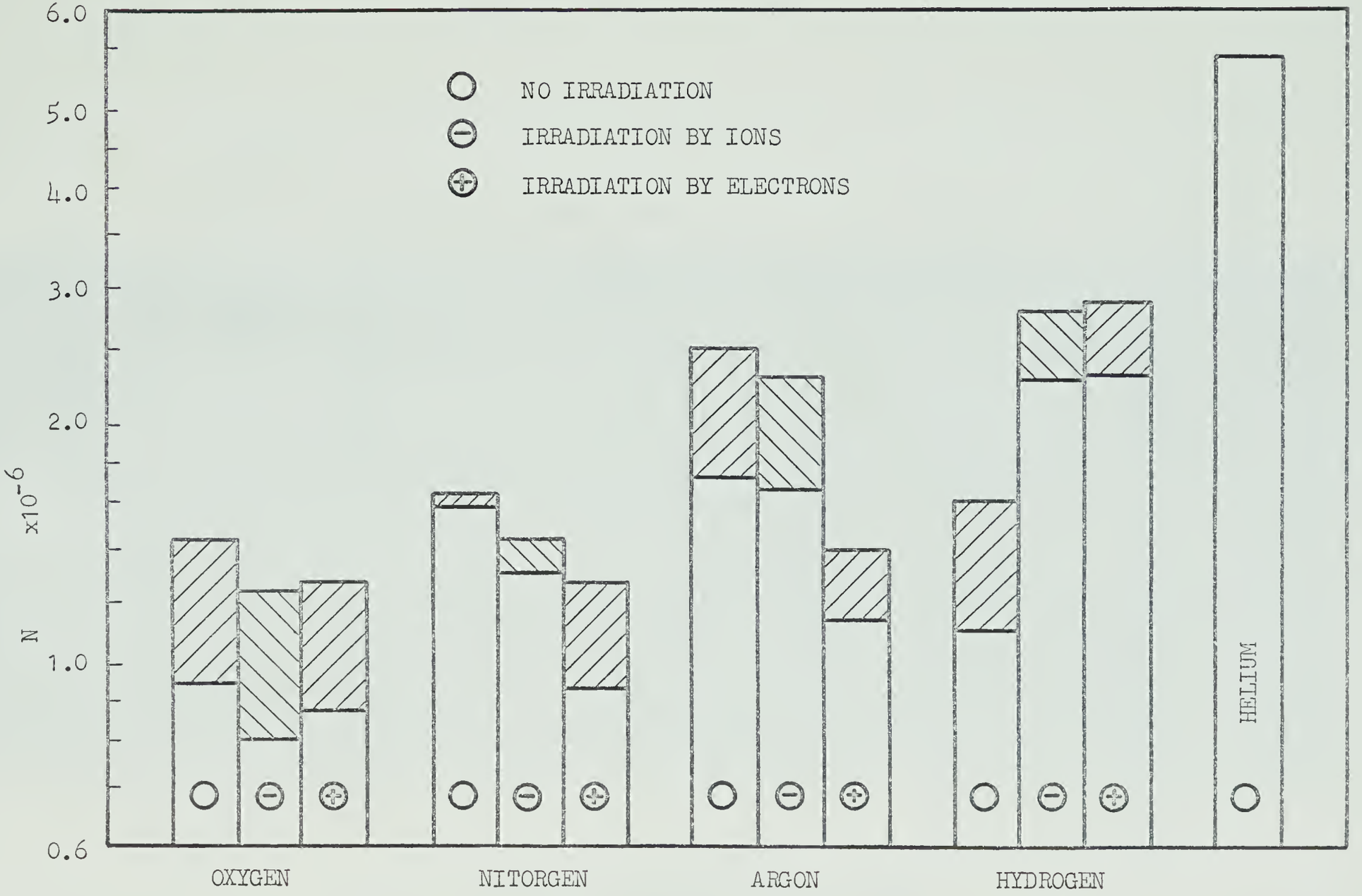

FIG. 8 Effect of environment on fatigue life.
Crosshatched area denotes scatter.

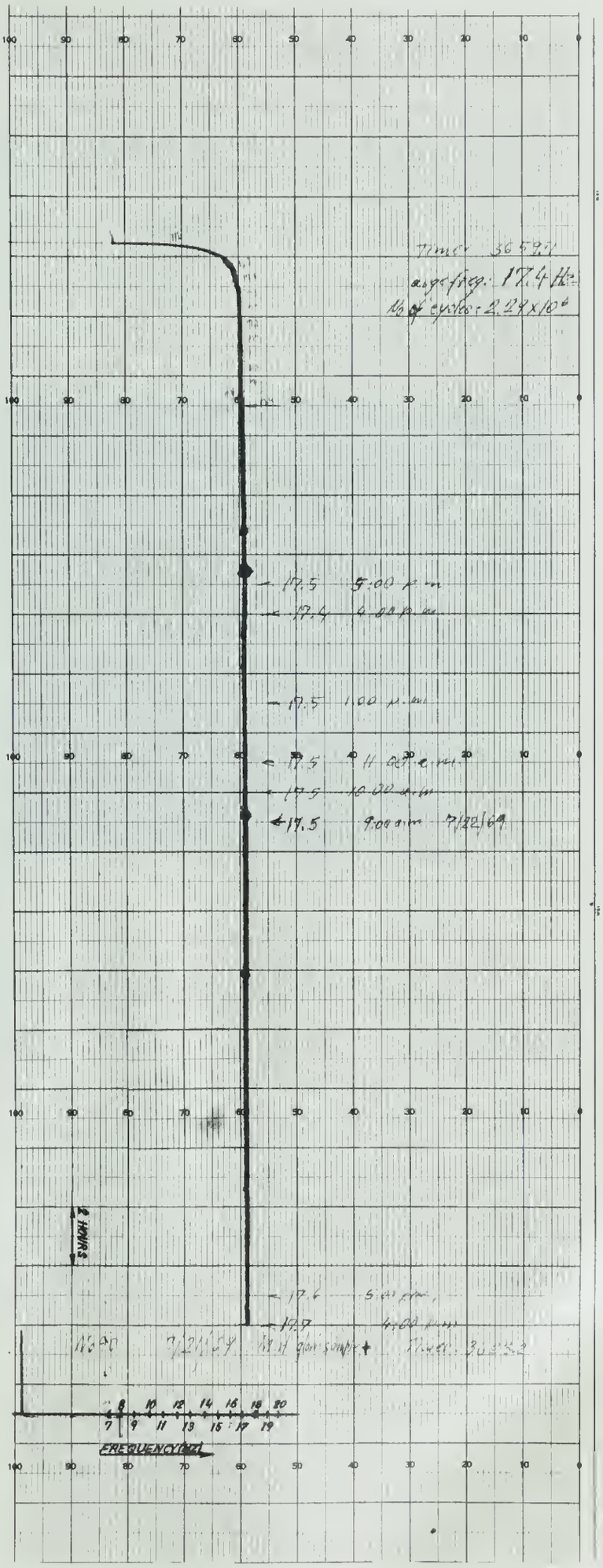

FIG. 9 Resonance frequency-time recording.

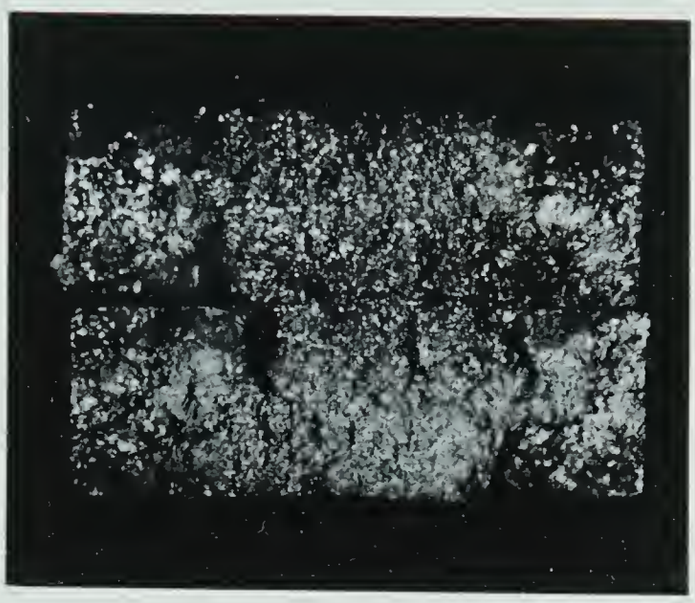

FIG. 10 Typical fracture surface. x18

FIG. 11 Fracture surface produced in oxygen.
Two-stage replica x1800

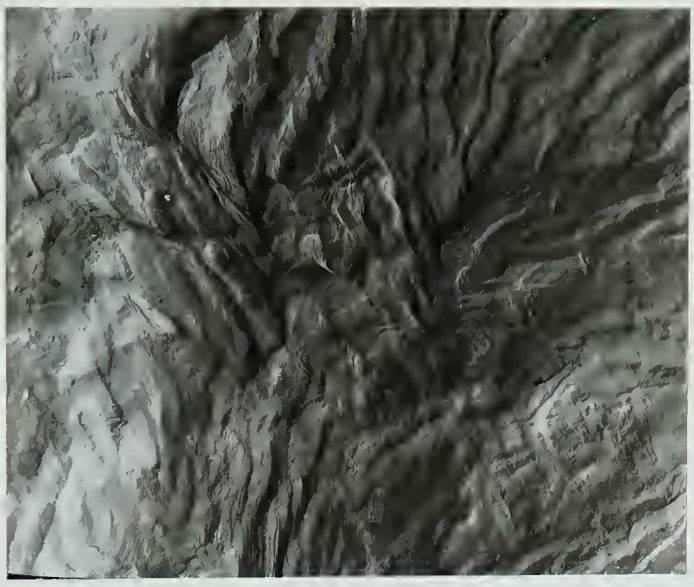

FIG. 12 Fracture surface produced in oxygen.
Two-stage replica x2800

FIG. 13 Fracture surface produced in oxygen.
Two-stage replica x550

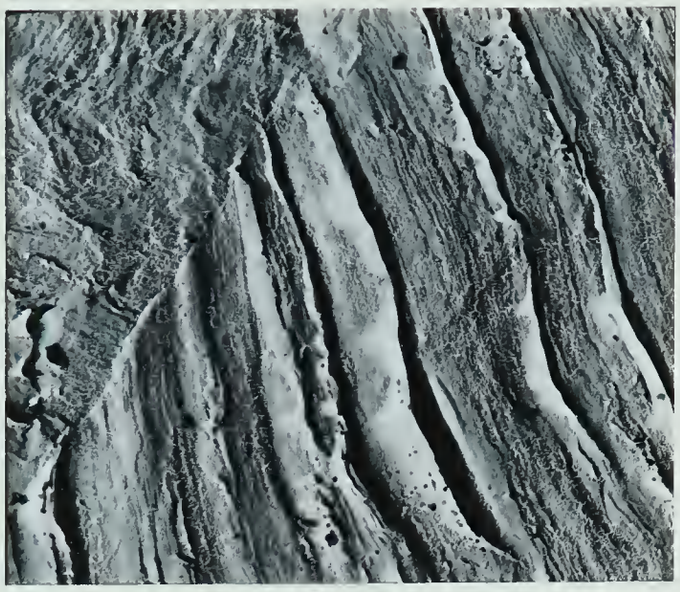

FIG. 14 Fracture surface produced in oxygen.
Two-stage replica x8000

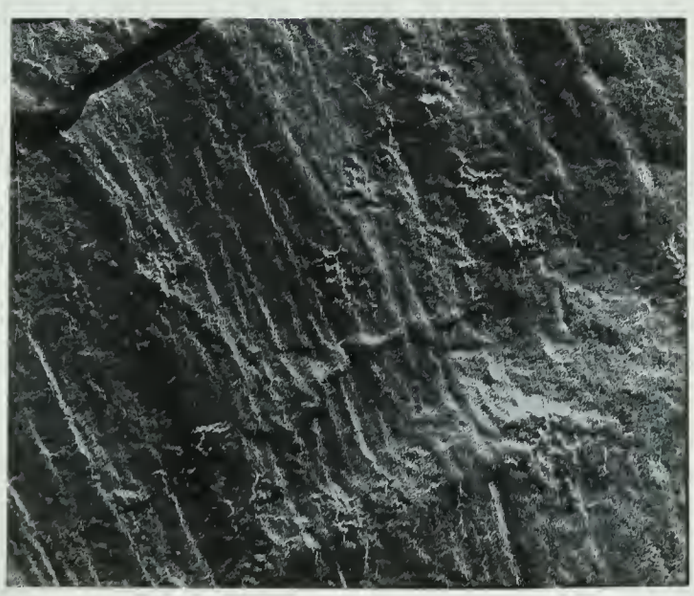

FIG. 15 Fracture surface produced in oxygen.
Two-stage replica x29000

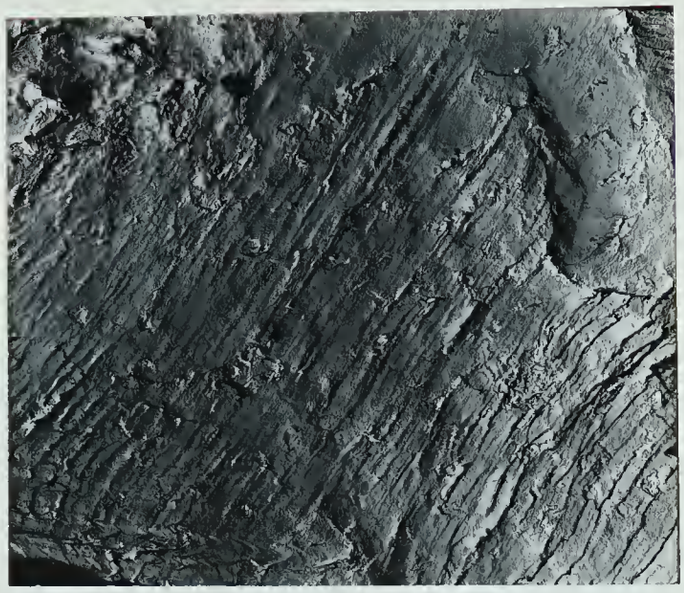

FIG. 16 Fracture surface produced in oxygen under irradiation by ions. Two-stage replica x3000

FIG. 17 Fracture surface produced in oxygen under irradiation by electrons. Two-stage replica x3000

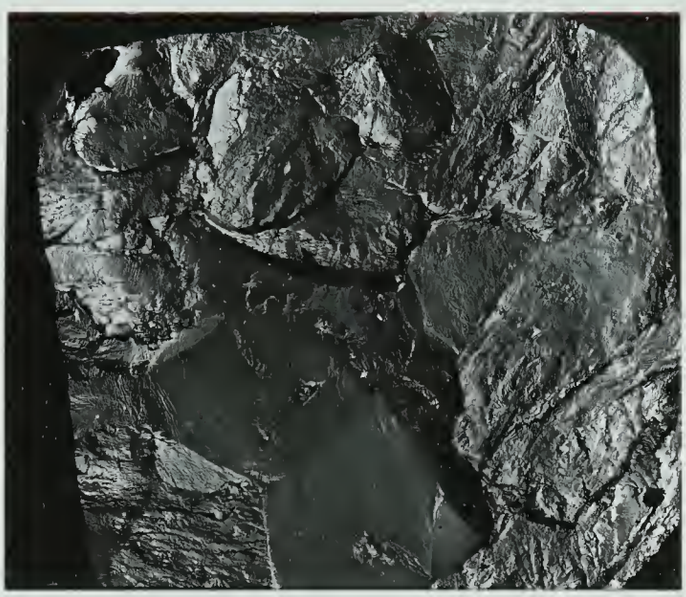

FIG. 18 Fracture surface produced in nitrogen under irradiation by ions. Two-stage replica x550

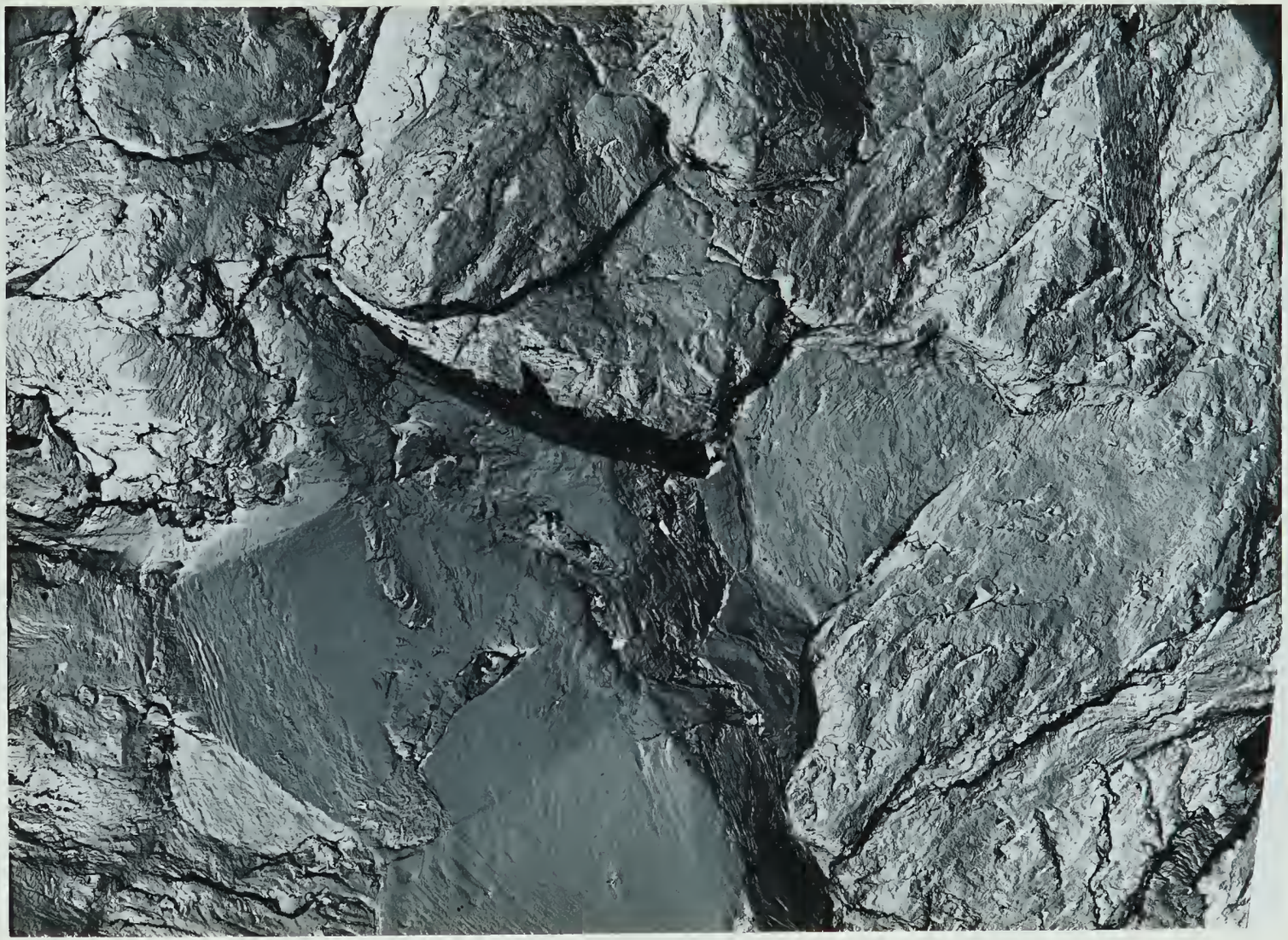

FIG. 19 Fracture surface produced in nitrogen under irradiation by ions.
Two-stage replica x1200

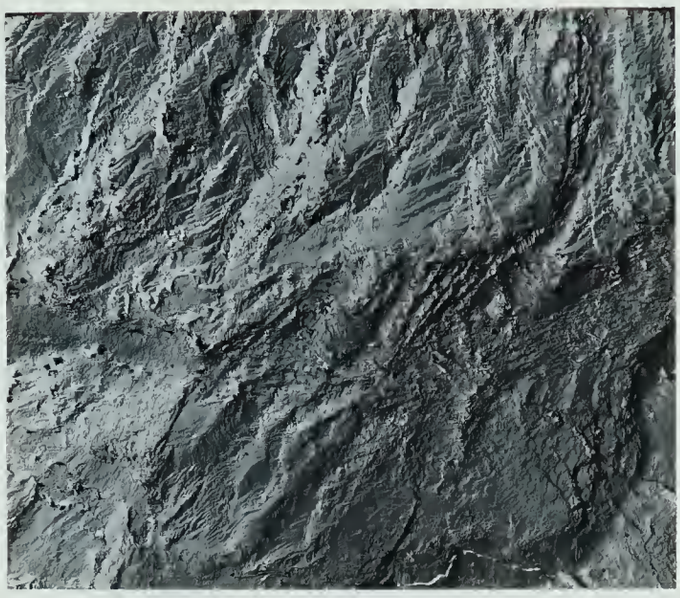

FIG. 20 Fracture surface produced in nitrogen under irradiation by ions. Two-stage replica x800

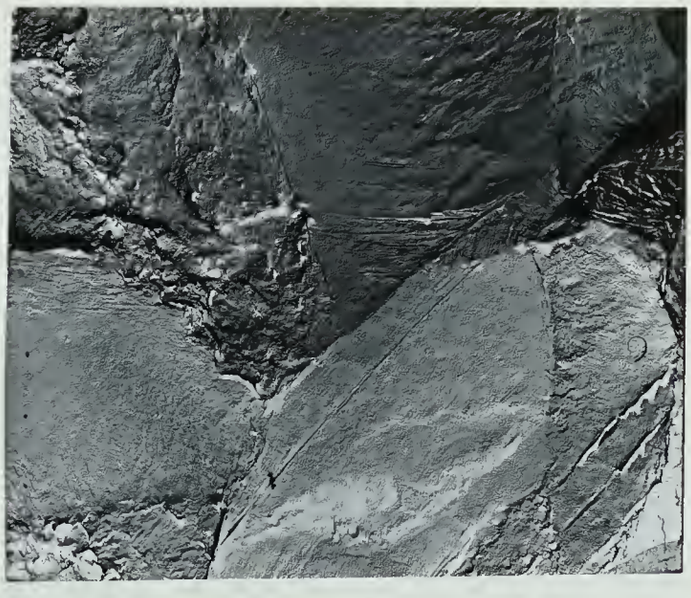

FIG. 21 Fracture surface produced in nitrogen under irradiation by electrons. Two-stage replica x800

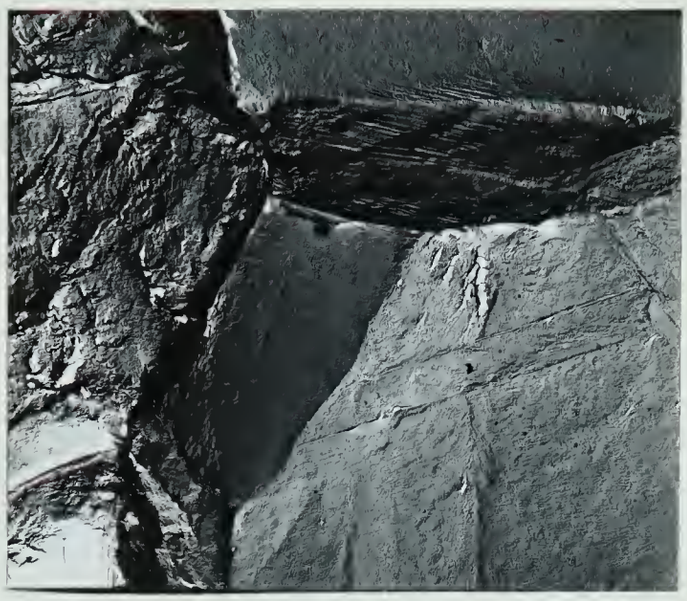

FIG. 22 Fracture surface produced in argon.
Two-stage replica x800

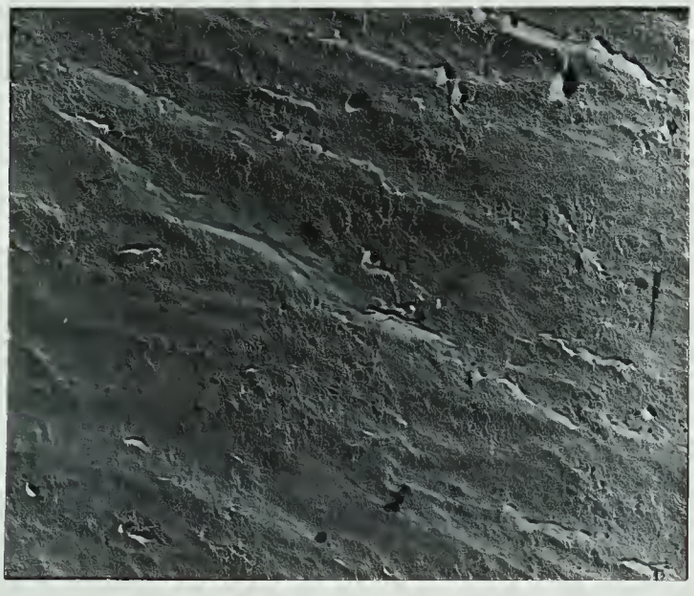

FIG. 23 Fracture surface produced in argon.
Two-stage replica x12000

FIG. 24 Fracture surface produced in argon.
Two-stage replica x3000

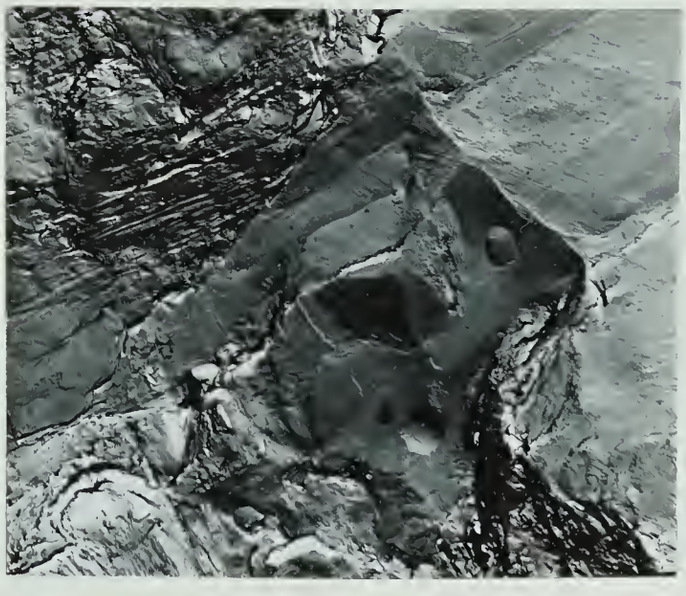

FIG. 25 Fracture surface produced in hydrogen.
Two-stage replica x3000

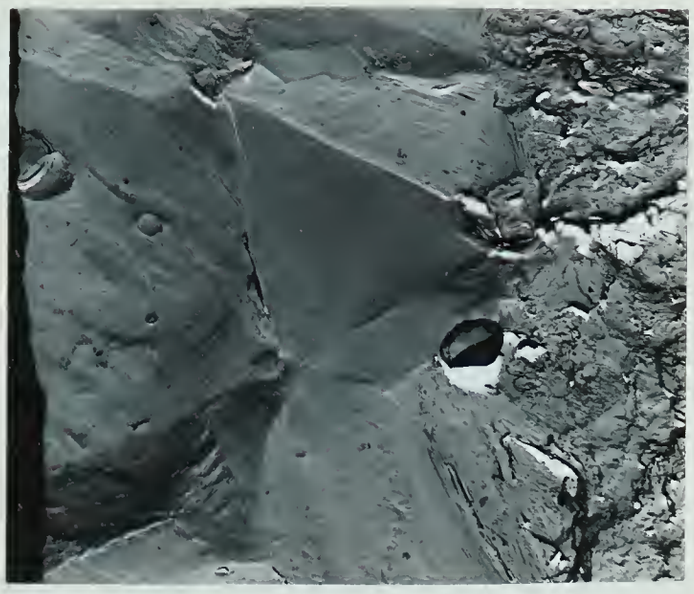

FIG. 26 Fracture surface produced in hydrogen.
Two-stage replica x3000

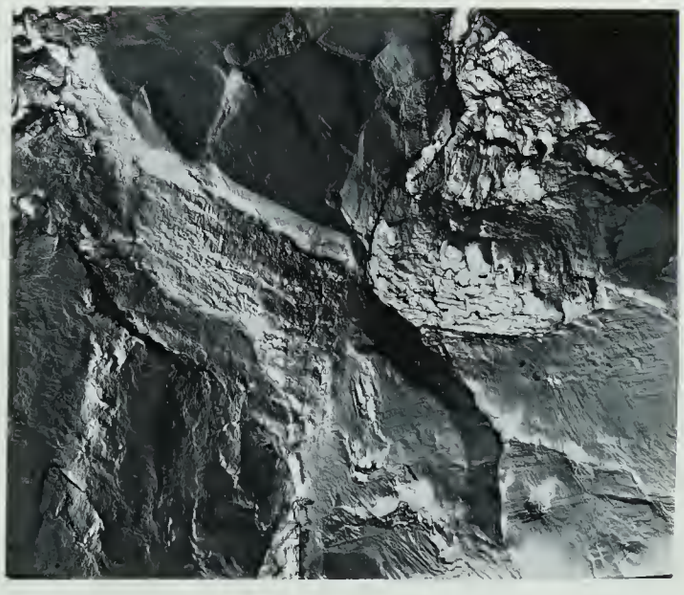

FIG. 27 Fracture surface produced in humidified air.
Two-stage replica x800

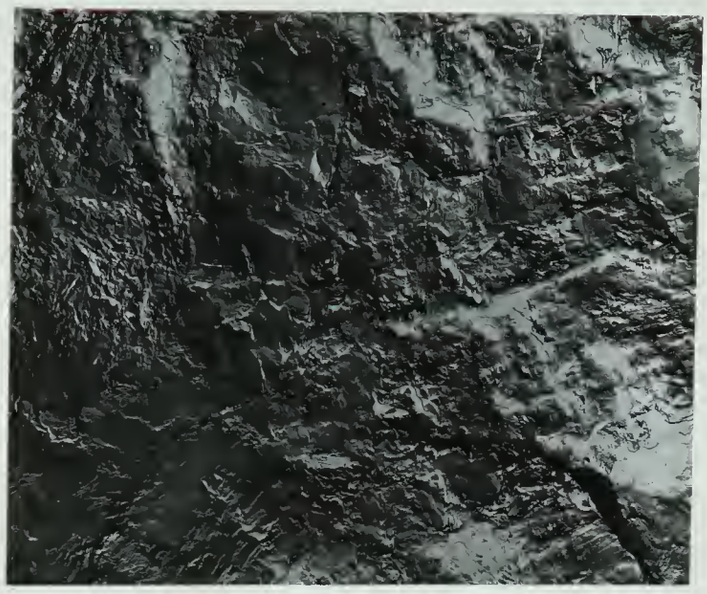

FIG. 28 Fracture surface produced in helium.
Two-stage replica x1200

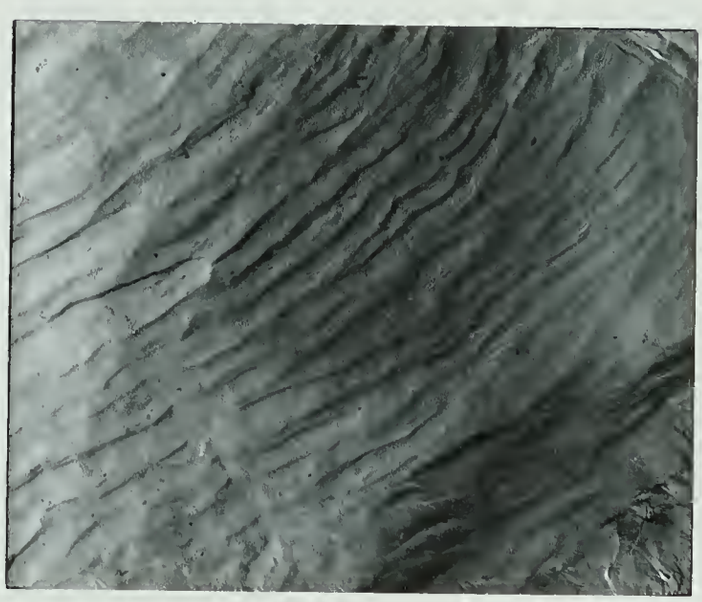

FIG. 29 Fracture surface produced in helium.
Two-stage replica x2800

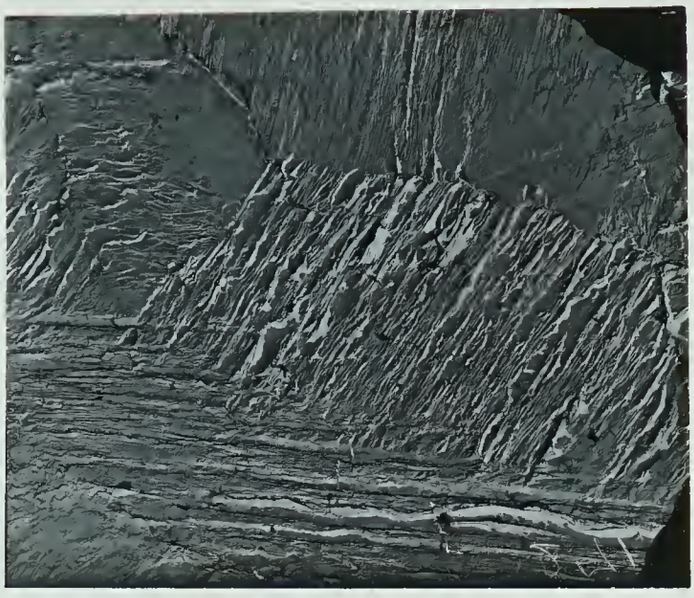

FIG. 30 Free surface produced in helium.
Two-stage replica x800

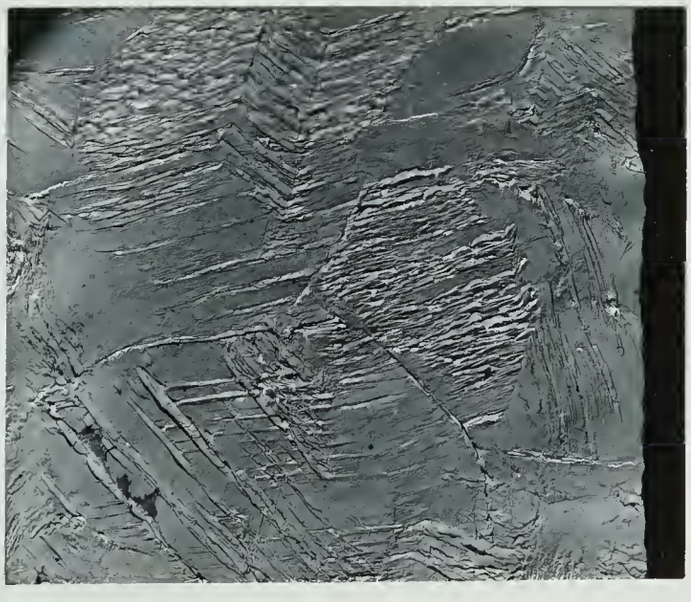

FIG. 31 Free surface produced in oxygen.
Two-stage replica x550

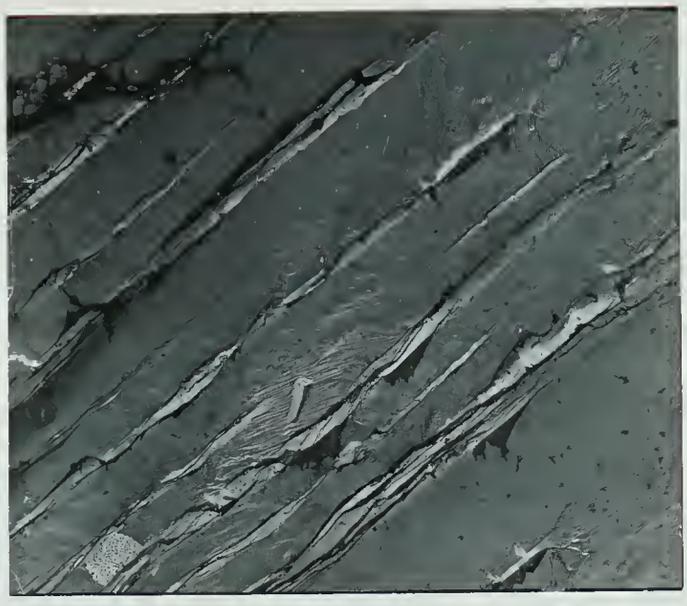

FIG. 32 Free surface produced after 6 hours in oxygen.
Two-stage replica x800

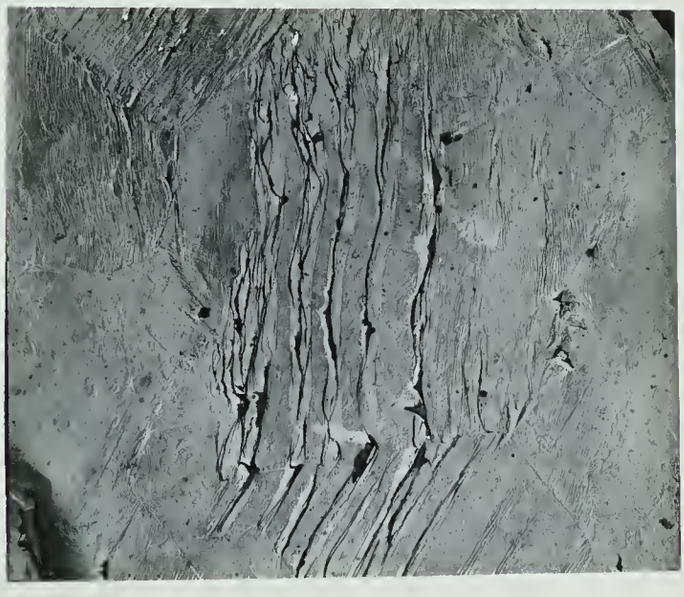

FIG. 33 Free surface produced after 3 hours in oxygen.
Two-stage replica x800

FIG. 34 Free surface produced after 3 hours in helium.
Two-stage replica x800

FIG. 35 Free surface produced after 3 hours in helium.
Two-stage replica

x1800

FIG. 36 Free surface of an unfatigued specimen. Two-stage replica x800

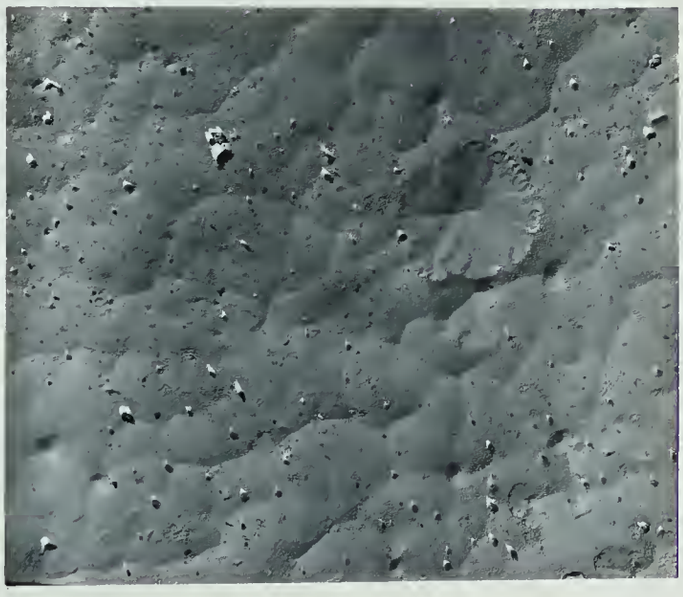

FIG. 37 Free surface produced in argon under irradiation by ions. Two-stage replica x800

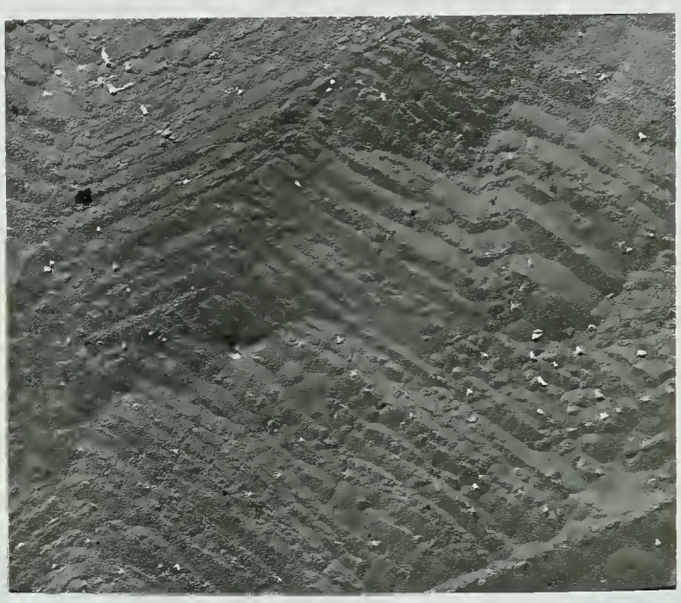

FIG. 38 Free surface produced in nitrogen under irradiation by ions. Two-stage replica x800

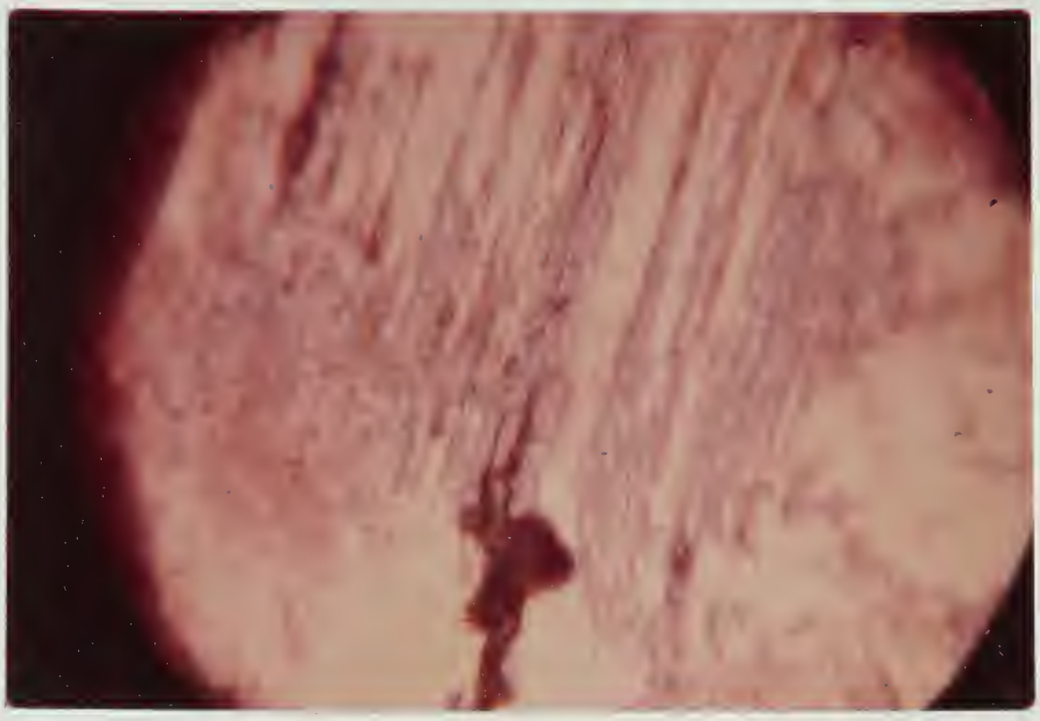

FIG. 39 Free surface produced in oxygen under irradiation by ions. Optical micrograph x900

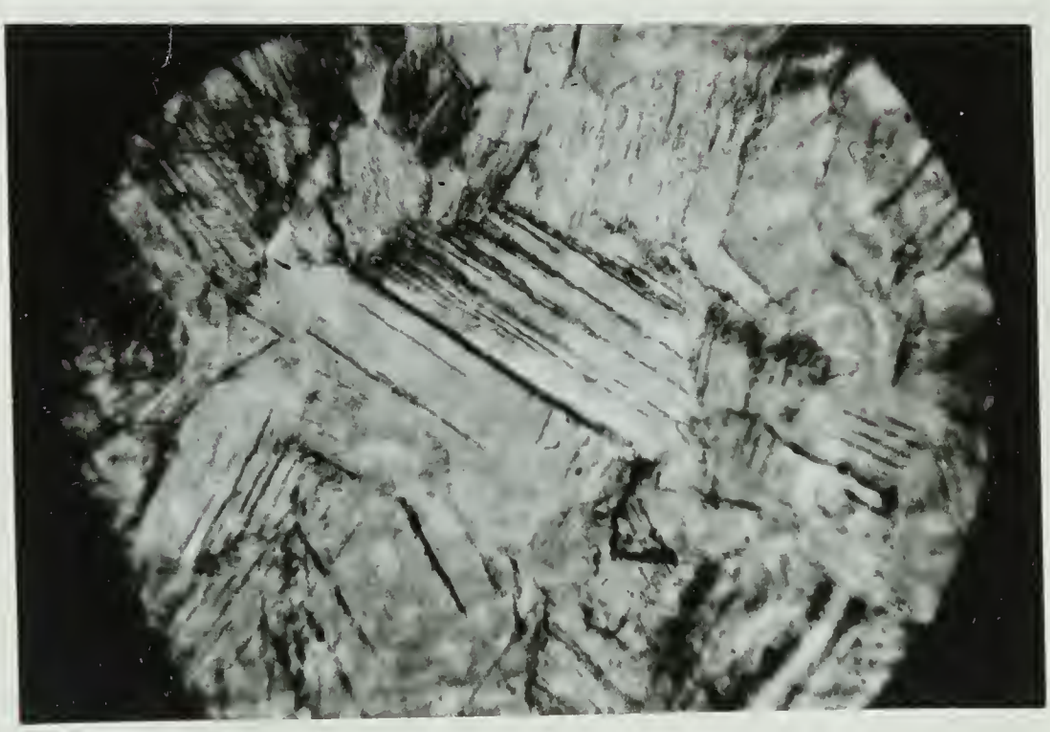

FIG. 40 Free surface produced in oxygen. Optical micrograph x500

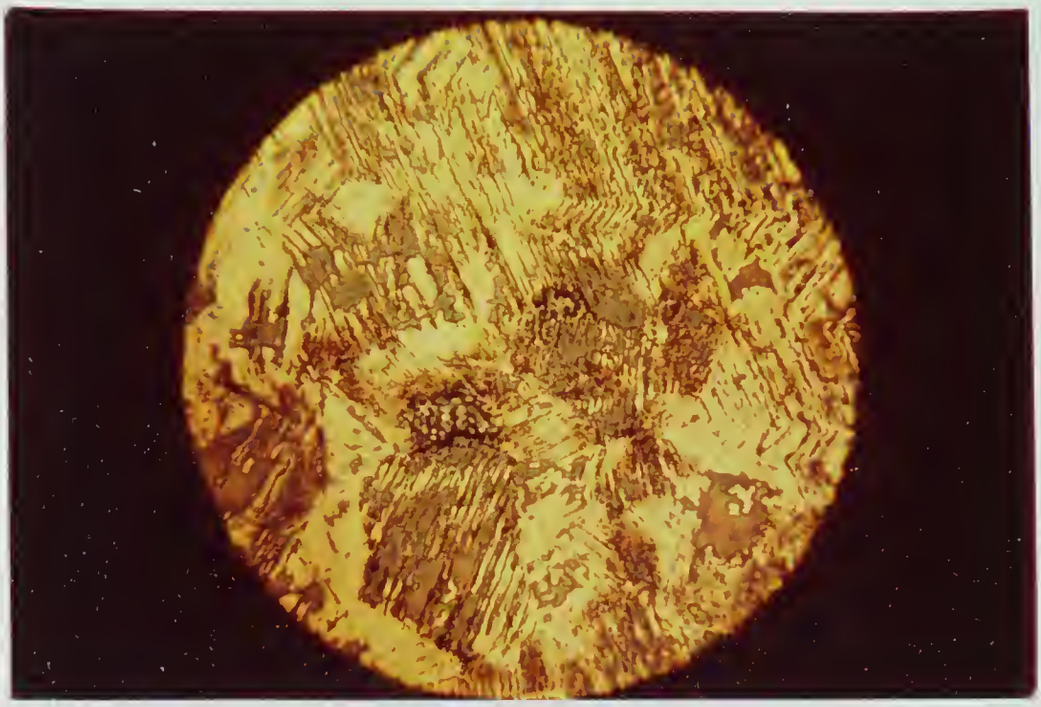

FIG. 41 Free surface produced in oxygen under irradiation by ions. Optical micrograph x350

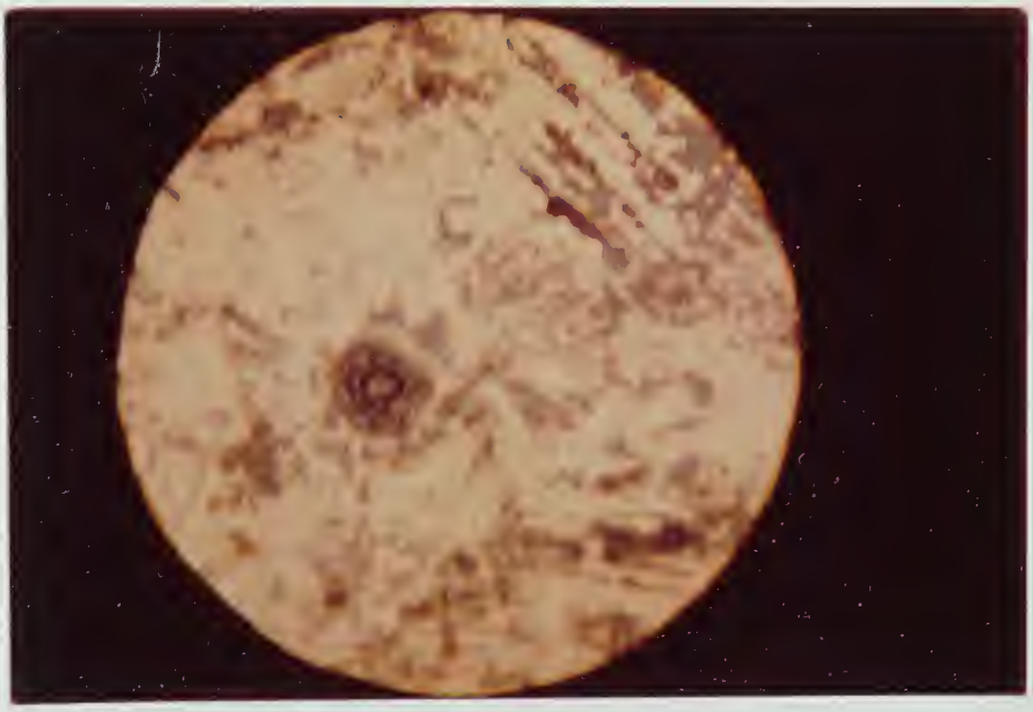

FIG. 42 Free surface produced in oxygen under irradiation by ions. Optical micrograph x350

FIG. 43 Free surface produced in oxygen under irradiation by ions. Optical micrograph x350

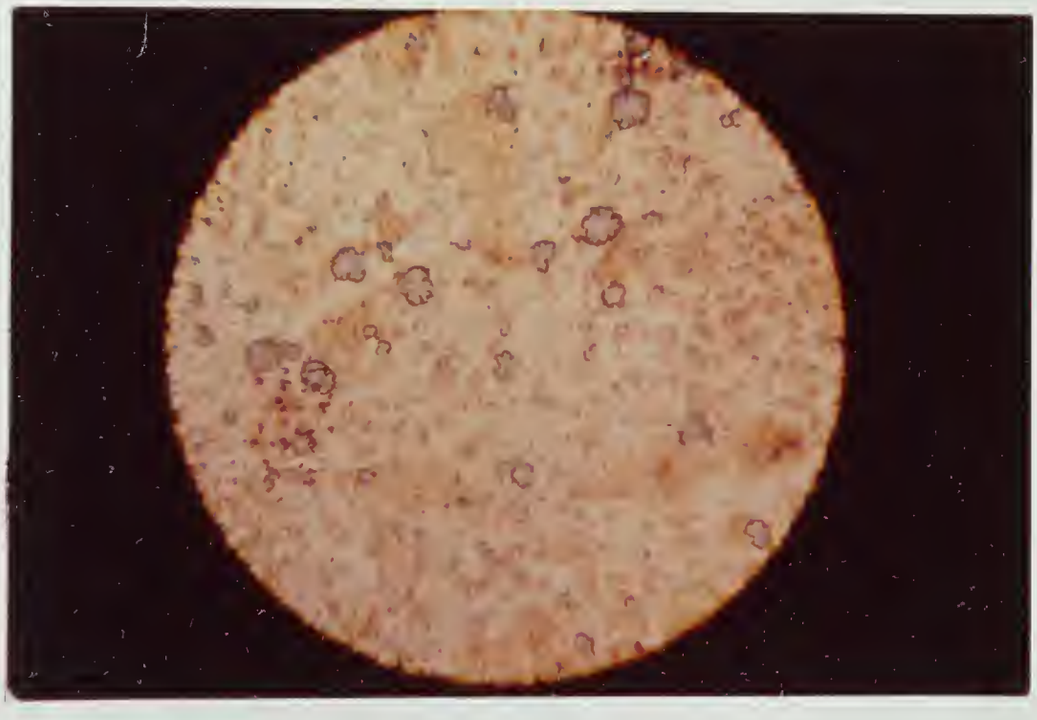

FIG. 44 Free surface produced in argon under irradiation by ions. Optical micrograph x350

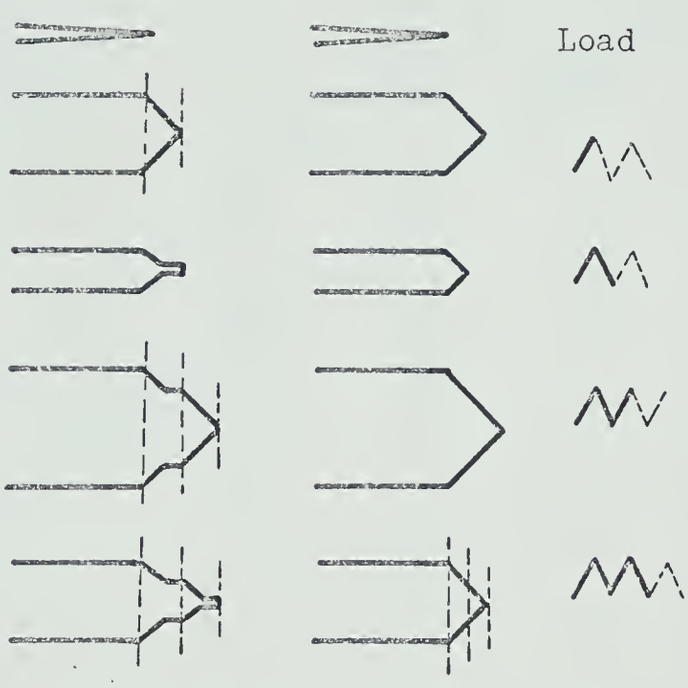

(a) No reversed slip (oxidation) (b) Reversed slip (vacuum)

FIG. 45 Model comparing crack tip extension after two load cycles in air and in vacuum. (After Pelloux (10).)

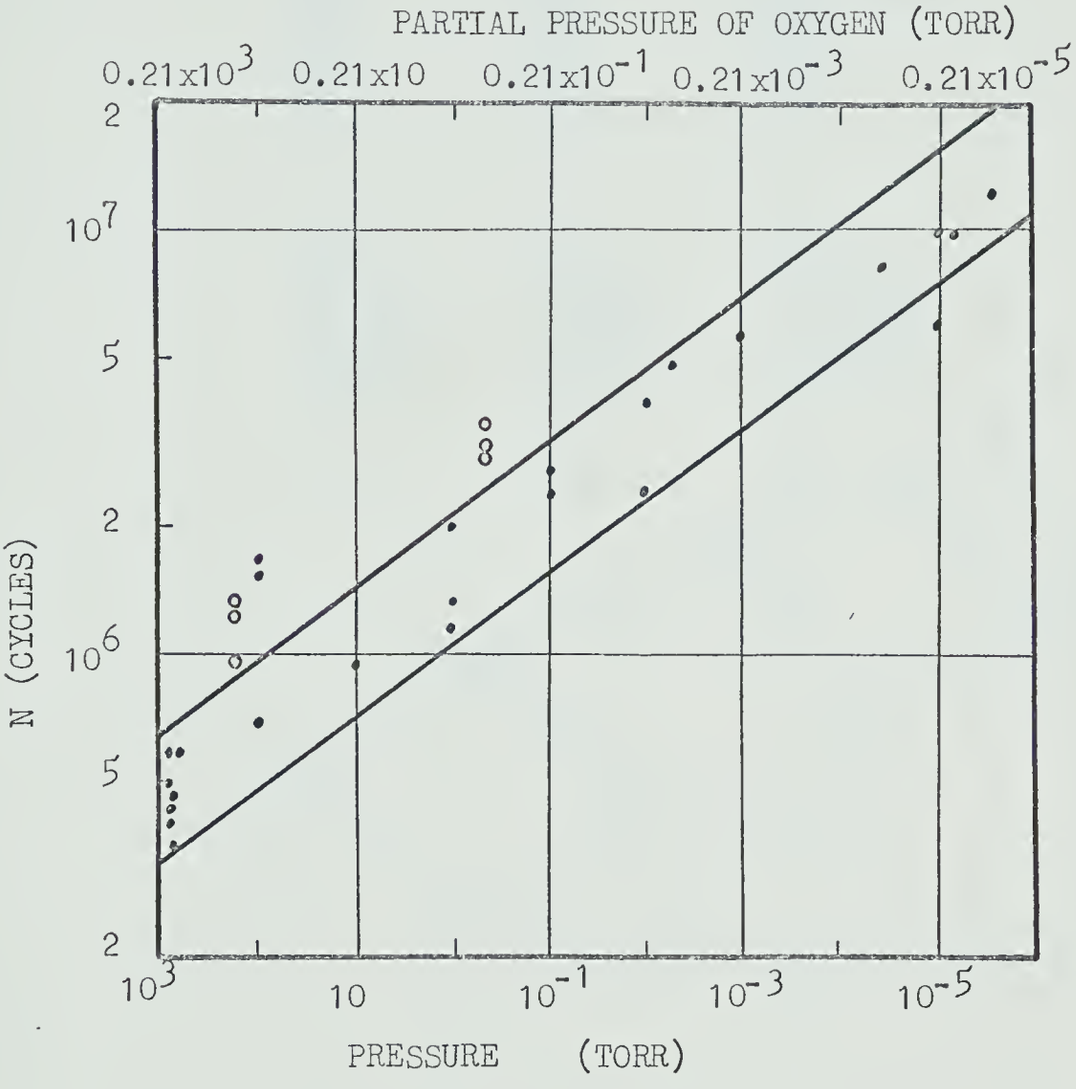

FIG. 46 Variation of fatigue life of copper with air and with oxygen pressure.
(• data obtained by Wadsworth and Hutchings (6))
(o data obtained in this project)

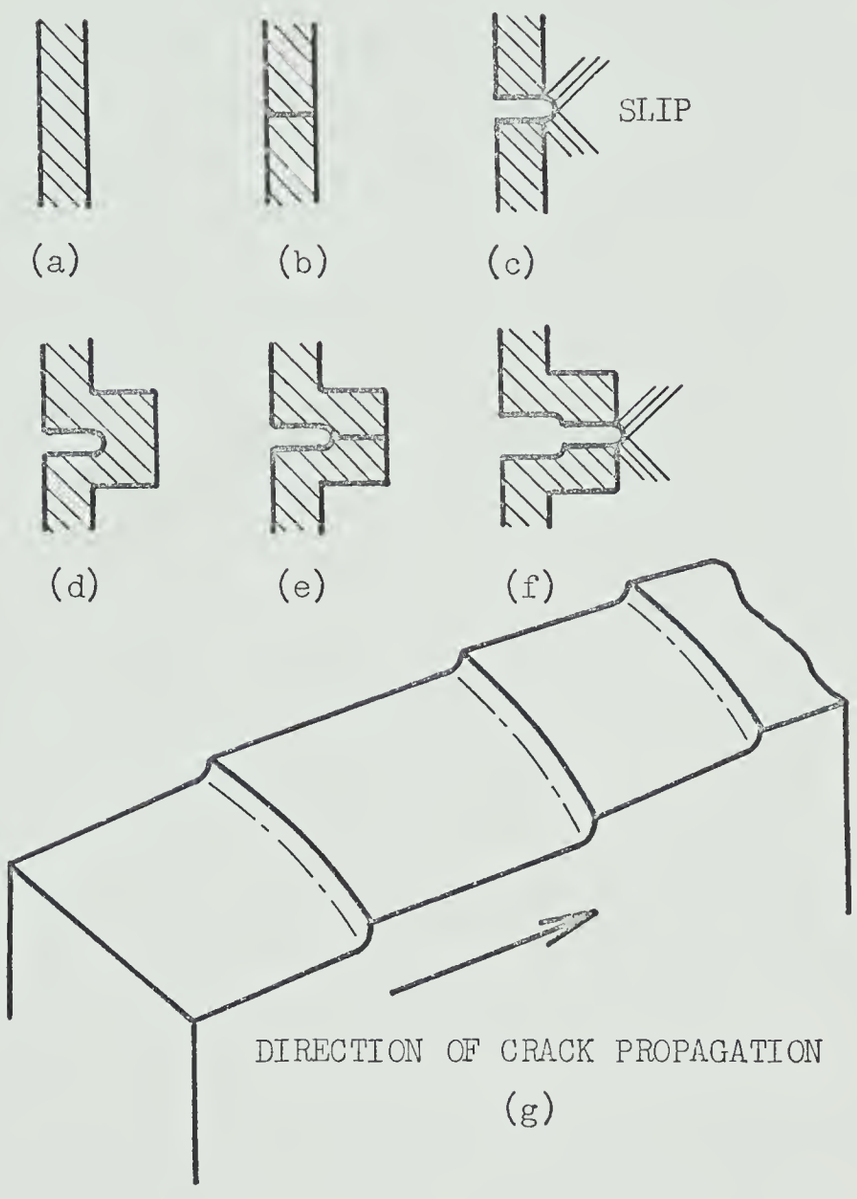

FIG. 47 (a) through (f). Mechanism of brittle-film rupture; (g) resulting structure of fracture surface. (After Westwood (1).)